

UNIVERSITÉ DU QUÉBEC À MONTRÉAL

VARIABILITÉ DE LA TEMPÉRATURE DE SURFACE
ET DU COUVERT DE GLACE DE MER DANS LE DÉTROIT DE FRAM
AU COURS DES DEUX DERNIERS MILLÉNAIRES

MÉMOIRE
PRÉSENTÉ
COMME EXIGENCE PARTIELLE
DE LA MAÎTRISE EN SCIENCES DE LA TERRE

PAR
SOPHIE BONNET

MARS 2009

UNIVERSITÉ DU QUÉBEC À MONTRÉAL

VARIABILITY OF SEA-SURFACE TEMPERATURE
AND SEA-ICE COVER IN THE FRAM STRAIT
OVER THE LAST TWO MILLENNIA

THESIS
PRESENTED
AS PARTIAL REQUIREMENT FOR A
M.Sc. IN EARTH SCIENCES

BY
SOPHIE BONNET

MARCH 2009

UNIVERSITÉ DU QUÉBEC À MONTRÉAL
Service des bibliothèques

Avertissement

La diffusion de ce mémoire se fait dans le respect des droits de son auteur, qui a signé le formulaire *Autorisation de reproduire et de diffuser un travail de recherche de cycles supérieurs* (SDU-522 – Rév.01-2006). Cette autorisation stipule que «conformément à l'article 11 du Règlement no 8 des études de cycles supérieurs, [l'auteur] concède à l'Université du Québec à Montréal une licence non exclusive d'utilisation et de publication de la totalité ou d'une partie importante de [son] travail de recherche pour des fins pédagogiques et non commerciales. Plus précisément, [l'auteur] autorise l'Université du Québec à Montréal à reproduire, diffuser, prêter, distribuer ou vendre des copies de [son] travail de recherche à des fins non commerciales sur quelque support que ce soit, y compris l'Internet. Cette licence et cette autorisation n'entraînent pas une renonciation de [la] part [de l'auteur] à [ses] droits moraux ni à [ses] droits de propriété intellectuelle. Sauf entente contraire, [l'auteur] conserve la liberté de diffuser et de commercialiser ou non ce travail dont [il] possède un exemplaire.»

AVANT-PROPOS

Ce mémoire de maîtrise est rédigé sous forme d'un article scientifique qui sera soumis à la revue *Marine Micropaleontology*. Par conséquent, la langue anglaise est utilisée et la mise en forme respecte les exigences de *Marine Micropaleontology* et non celle d'un mémoire de l'Université du Québec à Montréal. Les tableaux et les figures sont placés à la suite des références. Mme Anne de Vernal, chercheure et professeure au département des Sciences de la Terre et de l'Atmosphère de l'UQÀM a participé à la rédaction de cet article.

REMERCIEMENTS

Je remercie sincèrement ma directrice de recherche, Mme Anne de Vernal qui a su me donner ma chance quand je suis arrivée au Canada en m'accueillant dans son laboratoire. Elle m'a fait découvrir un domaine de recherche passionnant et m'a donné l'envie de continuer. Aussi, elle m'a permis de mieux connaître le milieu de la recherche scientifique en participant, entre autres, à différents congrès internationaux et à une campagne océanographique dans le détroit de Fram en Août 2008. Ses encouragements et sa disponibilité, malgré un emploi du temps très chargé, m'ont été très précieux. Je la remercie également pour son soutien financier. Un énorme merci à Maryse Henry, technicienne, et Taoufik Radi, post-doctorant, au GEOTOP, pour leur aide, conseils, soutien, enthousiasme et patience. Je remercie les étudiants, les chercheurs et le personnel du GEOTOP qui m'ont aidée tout au long de la maîtrise, notamment Claude Hillaire-Marcel et Bassam Ghaleb pour leur aide dans la chronologie et le ^{210}Pb et Linda Genovesi "Œil de Lynx" pour la lecture finale. Finalement, un merci tout particulier à ma mère qui m'a toujours motivée et soutenue tout au long de mes études.

TABLE DES MATIÈRES

AVANT-PROPOS.....	iii
REMERCIEMENTS.....	iii
LISTE DES FIGURES.....	vi
LISTE DES TABLEAUX.....	ix
RÉSUMÉ.....	x
INTRODUCTION GÉNÉRALE.....	1
CHAPITRE I	
VARIABILITY OF SEA-SURFACE TEMPERATURE AND SEA-ICE COVER IN THE FRAM STRAIT OVER THE LAST TWO MILLENNIA.....	10
Abstract.....	11
1. Introduction.....	12
2. Modern oceanic setting.....	13
3. Material and methods.....	15
4. Results	
4.1. Dinocyst assemblages in surface sediments from the Nordic Seas.....	18
4.2. Core JM04	
4.2.1. Chronology.....	19
4.2.2. Dinocyst record.....	20
4.2.3. Quantitative reconstructions of sea-surface conditions.....	22
5. Discussion.....	24
6. Conclusion.....	27
7. Acknowledgements.....	28
8. References.....	28

CONCLUSION GÉNÉRALE.....	52
--------------------------	----

APPENDICE A

TABLEAUX DE COMPTAGES ET CONCENTRATIONS DES PALYNOMORPHES TERRESTRES ET MARINS DE LA CAROTTE JM-06-WP-04-MCB.....	55
--	----

APPENDICE B

TABLEAUX DE COMPTAGES ET CONCENTRATIONS DES PALYNOMORPHES TERRESTRES ET MARINS DES ÉCHANTILLONS DE SURFACE DES MERS NORDIQUES (PROFONDEUR : 0-1 CM).....	63
--	----

BIBLIOGRAPHIE GÉNÉRALE.....	69
-----------------------------	----

LISTE DES FIGURES

Figure 1. Location of core JM-06-WP-04-MCB (JM04; 78.92°N, 6.77°E, water depth: 1497 m, core length: 54 cm) and trajectories of main ocean surface currents (cf. Hansen and Østerhus, 2000). Thick arrows depict warm currents and thin arrows, cold currents. Respectively, the dashed line and dotted line represent the Arctic and Polar Front, which are associated to the maximum sea-ice extension in winter and summer as defined from the 1953-2001 data set provided by the National Snow and Ice Data Center (NSIDC, 2001). Isobaths correspond to 200, 1000 and 3000 m. EGC: East Greenland Current, EIC: East Icelandic Current, ESC: East Spitsbergen Current, NC-E: eastern branch of the Norwegian Current, NC-W: western branch of the Norwegian Current, WSC: West Spitsbergen Current, NAC-S: southern branch of the North Atlantic Current, IC: Irminger Current.....36

Figure 2. Location map of the surface sediment samples used for canonical correspondence analysis (cf. Figure 6). Diamonds: data from de Vernal et al. (2005); circles: data from new reference sites (cf. Table 1). Isobaths correspond to 200, 1000 and 3000 m.....37

Figure 3. a) Modern sea-ice cover with concentration greater than 50% as a function of years AD at the site of core JM04 (black curve). Data from 1953 to 2001 are provided by the NSIDC (2001). On the left, the histogram represents historical records of sea-ice cover with concentration greater than 30% as a function of years AD with a 30-year average (AD 1596 to 2002). On the right, the grey curve illustrates historical records for the period AD 1953-2002. Data are compiled from ACSYS (2003). Note the important variability of sea-ice cover and its absence since 1982. **b)** Historical sea-ice records for the period AD 1900-2002 and mean annual (black curve) and mean winter (December to March; grey curve) air temperature anomalies (°C) between 1901 and 1995 in this area (75-80°N; 5-11°E). Annual and winter temperatures are, respectively, $-8.35 \pm 1.57^{\circ}\text{C}$ and $-16.03 \pm 2.92^{\circ}\text{C}$38

Figure 4. Location map of surface sediment samples used to reconstruct past sea-surface conditions from dinocyst assemblages in core JM04. **a)** Reference database used for MAT (n=1208 sites). **b)** Calibration databases for ANN: one includes all sites from the North Atlantic and Arctic (n=735 sites). The other one includes sites from the area delimited by the dashed line (n=437 sites), as defined from the best analogues selected using MAT (red points).....40

Figure 5. Percentage diagram of dinocyst taxa in surface sediment samples ranked by latitude (cf. Figure 2 for location). Different scales were used for dominant and accompanying taxa. Percentages of taxa with occasional occurrence lower than 1% are not reported. Dinocyst concentrations and modern sea-surface conditions (cf. National Ocean Data Center (NODC) and NSIDC, 2001) are indicated on the right of the diagram.....41

Figure 6. Results of CCA analysis. Ordination diagram of dinocyst taxa and environmental variables according to axis 1 and 2, and Pearson cross-correlation matrix between these two axes and hydrographical parameters. This analysis was performed with the XLSTAT software (Addinsoft, 2008), using the 94 sites (cf. Figure 2).....42


Figure 7. Geographical distribution of the scores for CCA axes 1 and 2, which represent, respectively, 77.27% and 12.81% of the total variance. Isobaths correspond to 200, 1000 and 3000 m.....43

Figure 8. a) Ln Lead-210 excess and Cesium-137 activities as a function of depth in core JM04. b) Age model of core JM04. The five dots with error bars represent calibrated Carbon-14 ages (see Table 2). The black line shows the interpolated ages vs. depth relationship, which was used to establish the chronology in the core (Figures 9, 10 and 12). From 11.5 cm to the base of the core, we calculate mean sedimentation rate of 18 cm/kyrs. The close-up of depth vs. age for the upper 12 cm of the core shows the age model based on Lead-210. c) Percentage of the coarse sand fraction ($>106\ \mu\text{m}$) as a function of age.....44

Figure 9. a) Diagram of dinocyst taxa percentages as a function of age in core JM04. Different scales were used for dominant and accompanying taxa. Two assemblage zones separated by the horizontal dashed line were defined on the basis of the principal component analysis calculations (cf. Figure 10). b) Dinocyst concentrations (solid line) and fluxes (dotted line). The thick dashed line correspond to smoothed concentration values (three-point running average).....45

Figure 10. Principal components 1 and 2 (PC 1 and PC 2) as a function of age (left) and ordination diagram of dinocyst taxa based on PC 1 and PC 2 (right) for core JM04.....46

Figure 11. Distribution maps of *Selenopemphix quanta*, *Spiniferites mirabilis-hyperacanthus* and *Impagidinium sphaericum* in surface sediment samples of the northern North Atlantic. Occurrences are expressed in percentages. Isobaths correspond to 200, 1000 and 3000 m.....47

Figure 12. Reconstruction of sea-surface conditions (temperatures, salinity, sea-ice cover) from dinocyst assemblages for the last 2500 years as a function of age, based on MAT and ANN techniques. The overall reference database (n=1208 sites) was used for MAT (red line), the North Atlantic and Arctic database with n=735 sites was used for ANN (blue line) as well as the database delimited by the analogues with n=437 sites (dashed line) (cf. Figure 4 for calibration databases). The modern values with their standard deviations are represented by 48

LISTE DES TABLEAUX

Table 1. Location of surface sediment samples analyzed in the present study and core JM04.....	49
Table 2. Radiocarbon ages from core JM04. The software Calib 5.0.2 (Stuiver et al., 2000) was used for calibration with a reservoir correction of 400 years and normalization for a $\delta^{13}\text{C}$ of -25‰ PDB (Stuiver et al., 2000).....	49
Table 3. Results of validation tests of sea-surface temperatures, salinity and sea-ice cover reconstructions based on MAT and ANN (databases of Atlantic+Arctic sites and according to the analogues). R^2 corresponds to the correlation coefficient between observed and estimated values. RMSE (Root Mean Square error) is the standard deviation of the difference between observed and estimated values. RMSEP (Root Mean Square Error of Prediction) is calculated by dividing the database in calibration and verification data sets.....	50
Table 4. Distance of the ten closest analogues for the core JM-06-WP-04-MCB as a function of depth, obtained with MAT. The threshold value for poor analogues is 1.31.....	51

RÉSUMÉ

Une carotte sédimentaire, couvrant les derniers 2500 ans, a été échantillonnée sur la marge continentale Ouest du Spitzberg dans le détroit de Fram (78,92°N 6,77°E, profondeur d'eau : 1497 m) avec pour objectif de reconstituer les variations hydroclimatiques à partir de l'analyse des assemblages de dinokystes. L'abondance relative des taxons de dinokystes ainsi qu'une analyse en composantes principales permet de distinguer une période de transition majeure à 300 ans cal. BP. Celle-ci est marquée par la disparition simultanée des taxons thermophiles *Spiniferites mirabilis-hyperacanthus* et *Impagidinium sphaericum* ainsi qu'une augmentation des taxons polaires-subpolaires *Impagidinium pallidum* et *Pentaparsodinium dalei*. Les températures de surface estimées suggèrent des conditions plus chaudes que celles de l'actuel (moyenne de 7°C en Été, soit une anomalie d'environ +2°C) jusqu'à 300 ans cal. BP malgré plusieurs phases de refroidissement vers 1700, 1500, 1200 et 800 ans cal. BP. Les derniers 300 ans se caractérisent par une tendance au refroidissement, avec des températures d'Été chutant de 7,6 à 3,5°C et un couvert de glace de mer atteignant 7 mois/an. Les résultats obtenus montrent que le couvert de glace de mer et la température de surface océanique dans la région du détroit de Fram sont sensibles aux variations hydroclimatiques, principalement liées au débit relatif des eaux chaudes et salées du courant Nord Atlantique pénétrant à l'Est et des eaux froides et déssalées sortant de l'Arctique, à l'Ouest. Nos données mettent également en évidence un optimum thermique vers 1320 ans cal. BP qui représenterait le seul intervalle des derniers 2500 ans pouvant être un analogue des conditions modernes post-AD 2000 et se singularisant par une absence du couvert de glace de mer.

Mots clés : Holocène, mers nordiques, détroit de Fram, conditions océaniques de surface, dinokyste

INTRODUCTION GÉNÉRALE

Changement climatique et instabilités du climat Holocène

Les observations climatiques et hydrographiques de ces dernières décennies nous ont montré à quel point le climat est sensible aux moindres perturbations. Le dernier rapport du groupe d'experts intergouvernemental sur l'évolution du climat (GIEC, 2007) met en évidence ces instabilités climatiques et le fait que ce sont principalement les hautes latitudes qui enregistrent les changements les plus significatifs. En outre, les données satellitaires illustrent une diminution sans précédent dans l'étendue et la concentration du couvert de glace de mer arctique (*cf.* par exemple, <http://arctic.atmos.uiuc.edu/>). À l'échelle de l'Holocène, de nombreux travaux sur les hautes latitudes de l'hémisphère Nord confirment l'existence d'instabilités climatiques de basse fréquence. À titre d'exemple, en 1995, O'Brien démontra que la circulation atmosphérique au-dessus de la calotte groenlandaise variait en suivant des cycles millénaires (O'Brien *et al.*, 1995). D'autres études menées sur les carottes de glace du Groenland (GRIP : *Greenland Ice Core Project* et GISP 2 : *Greenland Ice Sheet Project Two*) ont confirmé ces instabilités avec des fluctuations séculaires à millénaires. Des observations semblables ont été faites à partir de divers enregistrements issus de carottes de glace (*e.g.*, Alley *et al.*, 1997), de spéléothèmes (*e.g.*, McDermott, Mattey et Hawkesworth, 2001), de la dendrochronologie (*e.g.*, MacDonald *et al.*, 2000 ; Bennike, 2004) et de carottes marines (*e.g.*, Bond *et al.*, 1997, 1999 ; Campbell *et al.*, 1998 ; Bianchi et McCave, 1999 ; Husum et Hald, 2004) (*cf.* Tableau et Figures des pages 5-9). Malheureusement, en raison de vitesses de sédimentation souvent faibles dans les milieux marins, notamment dans les régions arctiques et subarctiques, les reconstitutions paléocéanographiques manquent de résolution temporelle pour documenter les variations décennales à séculaires de l'Holocène (*e.g.*, Hald *et al.*, 2004).

Objectifs

Dans le contexte du réchauffement climatique actuel, il s'avère pertinent d'étudier les changements climatiques et océaniques récents, avec une résolution temporelle élevée, afin de mieux dissocier les cycles naturels des perturbations anthropiques. Ici, notre objectif est de développer un enregistrement haute résolution des variations hydroclimatiques pendant l'Holocène tardif dans le détroit de Fram, à partir de l'étude de la carotte JM-06-WP-04-MCB (JM04 dans le texte ; 78,92°N 6,77°E, profondeur d'eau : 1497 m, Figure 1). Celle-ci est localisée sur le talus de la marge continentale Ouest du Spitzberg où le sédiment holocène atteint plusieurs mètres d'épaisseur (Husum, 2006). Situé entre le Groenland et le Spitzberg, le détroit de Fram fait partie des mers nordiques, une des régions les plus importantes de l'Atlantique Nord puisqu'elle constitue une zone de convergence entre les masses d'eau des océans arctique et atlantique (Figure 1). Quelques études ont été menées dans cette région mais le manque de résolution ne permet pas de distinguer ces oscillations décennales à séculaires, en particulier pour l'Holocène tardif (*e.g.*, Hald *et al.*, 2004, 2007 ; Ślubowska-Woldengen *et al.*, 2007).

Contexte océanographique

Les mers nordiques se caractérisent par la rencontre des masses d'eaux chaudes et salées du courant Nord Atlantique (CNA), s'écoulant vers le Nord-Est, et les masses d'eaux froides et dessalées du courant Est Groenlandais (CEG), qui s'écoulent vers le Sud-Ouest. Le CNA, dans le prolongement du Gulf Stream, traverse l'Atlantique via la dérive Nord Atlantique et se poursuit par le courant Atlantique Norvégien puis le courant Ouest Spitzberg. Le CNA représente un débit de 35 Sv (Krauss *et al.*, 1987). En atteignant les hautes latitudes, celui-ci redistribue la chaleur latente accumulée au niveau de l'Équateur. Le CNA joue donc un rôle prépondérant sur le climat des régions polaires. Il joue également un rôle important sur la circulation thermohaline puisque son refroidissement hivernal rend compte de la

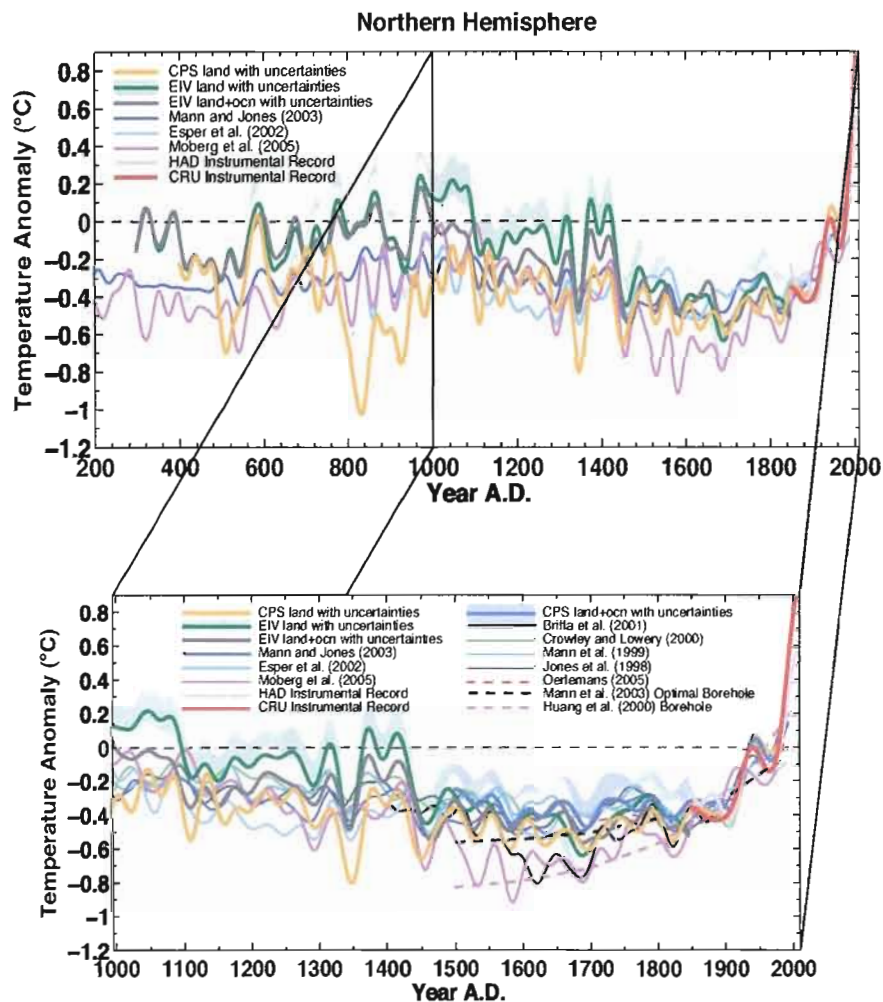
formation d'eau profonde dans les mers nordiques. La formation d'eau profonde dépend aussi de la densité et de la salinité des eaux de surface. Or, dans les mers nordiques, ces deux paramètres sont déterminés par les flux d'eau douce d'origine arctique. Le débit d'eau douce du détroit de Fram est estimé à environ 160 mSv réparti de la manière suivante : 80 mSv sous forme de glace et 65-95 mSv sous forme liquide (*cf.* Dickson *et al.*, 2007). Toutefois, la quantification de l'exportation de glace est différente selon les études et les paramètres pris en compte, sans doute en raison d'une variabilité interannuelle élevée. Par exemple, Koenigk *et al.* (2006) rapporte un flux sortant de glace de mer entre 75 et 100 mSv. Quoi qu'il en soit, le détroit de Fram semble être un secteur très sensible du système climatique, qu'il s'agisse du CNA ou des flux d'eau douce issus de l'Arctique.

Méthodes

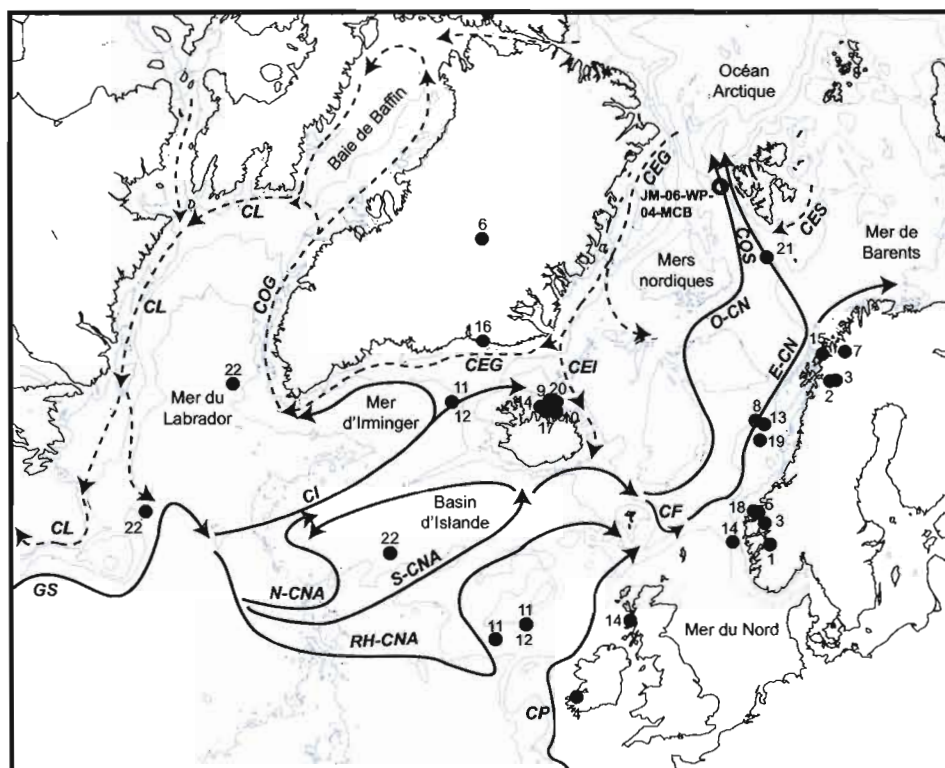
Les conditions océaniques de surface (température, salinité, glace de mer) de la carotte JM04 sont reconstituées en utilisant les kystes de dinoflagellés (*i.e.*, dinokystes) qui sont des protistes. Les dinokystes sont composés d'une paroi organique réfractaire nommée dinosporine (*e.g.*, Kokinos *et al.*, 1998 ; Versteegh et Blokker, 2004), ils présentent l'avantage de ne pas être affectés par la dissolution et la distribution de leurs assemblages est étroitement liée aux paramètres hydrographiques. Dans les environnements subpolaires, ils sont bien préservés dans les sédiments et leur diversité taxonomique est relativement élevée (de Vernal, Guiot et Turon, 1994 ; de Vernal *et al.*, 1997, 2001, 2005 ; de Vernal et Marret, 2007 ; Mudie et Rochon, 2001).

Dans le but de faire les meilleures reconstitutions possibles au site de carottage, nous avons augmenté le nombre d'échantillons de la base de données de référence des dinokystes dans les mers nordiques et le détroit de Fram à partir de l'analyse des échantillons de surface collectés lors des campagnes océanographiques *WarmPast* en 2006 et 2007 (JM06-WP et JM07-WP) (Figure 2) (Husum, 2006, 2007). La base de

données de référence des dinokystes dans les mers nordiques, présentée ici, comprend 94 sites au-dessus de 70°N. Elle a été utilisée pour analyser la distribution des assemblages à une échelle régionale et pour définir les relations avec les conditions hydrographiques modernes, le plus précisément possible (Figure 2). Ces données régionales ont été combinées avec la base de données Nord Atlantique et Arctique des dinokystes (de Vernal *et al.*, 2005) pour la reconstitution du couvert de glace, des températures et salinités de surface, à partir de la technique des analogues modernes (MAT) et de celle des réseaux artificiels de neurones (ANN) (*e.g.*, Guiot et de Vernal, 2007).



Graphique illustrant les anomalies de températures dans l'hémisphère Nord pour les derniers deux mille ans AD à partir d'observations, de reconstitutions et de simulations (figure empruntée au GIEC, 2007). La Période Chaude Médiévale et le Petit Âge Glaciaire sont définis entre AD 500-1500 et 1550-1850, respectivement (GIEC, 2007).



Carte de localisation de la carotte étudiée JM04 et des sites de l'Atlantique Nord auxquels il est fait référence dans le tableau. Les trajectoires des principaux courants de surface sont représentées (cf. Hansen et Østerhus, 2000). Les flèches épaisses et en tiretés correspondent, respectivement, aux courants chauds et froids. CEG : courant Est groenlandais, CEI : courant Est islandais, COG : courant Ouest groenlandais, CES : courant Est Spitzberg, CL : courant du Labrador, GS : Gulf Stream, CI : courant d'Irminger, N-CNA : branche Nord du courant Nord Atlantique, S-CNA : branche Sud du courant Nord Atlantique, RH-CNA : branche Rockall-Hatton du courant Nord Atlantique, CP : courant de pente, CF : courant des îles Féroé, E-CN : branche Est du courant norvégien, O-CN : branche Ouest du courant norvégien, COS : courant Ouest Spitzberg.

Tableau de synthèse des enregistrements paléoclimatiques de l'Holocène dans le domaine continental (voir Figure précédente pour la carte de localisation)

Numéro associé à la carte de localisation	Coordonnées	Auteurs	Site/région d'étude	Intervalle de temps étudié (année)	Résolution temporelle	Proxies utilisés	Paramètres étudiés	Périodicité(s) des événements	Amplitude des événements	Petit Âge Glaciaire (cal. BP)	Période Chaude Médievale (cal. BP)
1	60.55°N, 7.42°E	Dahl <i>et al.</i> , 1994	Norvège (Hardangerjøkulen)	9100-0	—	Dépôts terrestres et lacustres	Fluctuations des glaciers	—	—	575±75	—
2	Région autour de 68°N, 19°E	Grubb <i>et al.</i> , 2002	Suède	7400-0	Annuelle	Anneaux d'arbres (dendrochronologie)	Température d'été	De quelques années à plusieurs siècles, pas de variations millénaires	—	—	950-850
3	Région autour de 62.28°N, 6.65°E et 68.05°N, 18.22°E	Karlén et Kuylenstierna, 1996	Suède et Norvège	10 000-0	—	Sédiments glacio-lacustres et moraines alpines	Fluctuations des glaciers	2200 et 1000 ans	2°C	—	—
4	52.28°N, 9.43°W	McDermott <i>et al.</i> , 2001	Irlande (Crag Cave)	10 000-0	Décennale à 22 ans	Enregistrement $\delta^{18}O$ à partir d'un spéléothème	Température de l'air et composition isotopique de la vapeur d'eau	Pics centrés à 625, 169 et 78 ans	—	2 phases et est centré à 400	Centré à 1000±200
5	61.67°N, 7.17°E	Nesje <i>et al.</i> , 2001	Norvège (région de Jostedalsgreen)	10 500-0	13 à 118 ans avec une moyenne de 35 ans	Taille des grains dans les sédiments et porte au feu	Fluctuations des glaciers et précipitations hivernales	—	—	800	—
6	72.57°N, 38.48°W	O'Brien <i>et al.</i> , 1995	Groenland (GISP 2)	12 000-0	—	Flux du sel de mer et poussières terrestres	Composition chimique et circulation atmosphérique	2600 ans	—	—	—
7	69.2°N, 21.47°E	Seppä <i>et al.</i> , 2002	Fennoscandie (Toskajavri)	9600-0	60 ans	Pollen	Précipitations annuelles et température moyenne de Juillet	Pas de périodicité de 1500 ans, pas de changement abrupt du climat	< 2°C	800-200	1400-1000

Tableau de synthèse des enregistrements paléoclimatiques de l'Holocène dans le domaine océanique (voir Figure précédente pour la carte de localisation)

Numéro associé à la carte de localisation	Coordonnées	Auteurs	Site/région d'étude	Intervalle de temps étudié (année)	Résolution temporelle	Proxies utilisés	Paramètres étudiés	Périodicité(s) des événements	Amplitude des événements	Petit Âge Glaciaire (cal. BP)	Période Chaude Médievale (cal. BP)
8	66.97°N, 7.64°E	Andersson <i>et al.</i> , 2003	Mer de Norvège (Plateau de Voring)	3000-0	2 carottes : 3.4 et 8.4 ans	Isotopes stables et foraminifères planctoniques	Température de surface de l'océan	-	< 2°C	Commence vers 600-500, 2 phases et est centré à 300	1100-700
9	66.98°N, 17.95°W	Bendle <i>et al.</i> , 2007	Islande	10 200-0	20 ans	Alkénones	Température de surface de l'océan	Oscillations millénaires	> 2°C	340-80	-
10	56.35°N, 27.8°W	Bianchi et McCave, 1999	Islande	10 500-0	-	Taille moyenne des sils	Vitesse de l'ISOW (Iceland-Scotland Overflow Water)	1500 ans	-	Centré à 400	1050-750
11	64.78°N, 29.57°W 54.27°N, 16.78°W 54.25°N, 16.83°W 55.47°N, 14.72°W	Bond <i>et al.</i> , 2001	Détroit du Danemark (Plateau de Rockall)	12 000-0	30 à 50 ans	Débris glaciaires (vélage), foraminifères planctoniques, 8°C, verre volcanique d'Islande, grains d'hématite	Débris glaciaires (vélage)	1100-900 et 500-300 ans	-	-	-
12	64.78°N, 29.57°W 54.27°N, 16.78°W	Bond <i>et al.</i> , 1997	Détroit du Danemark (Plateau de Rockall)	11 100-1400	-	Débris glaciaires (vélage), foraminifères planctoniques, 8°C, verre volcanique d'Islande, grains d'hématite	Débris glaciaires (vélage)	1470±500 ans	< 2°C	-	-
13	66.97°N, 7.63°E	Calvo <i>et al.</i> , 2002	Mer de Norvège (Plateau de Voring)	15 800-0	7 à 200 ans	Alkénones	Température de surface de l'océan	1500 ans	Max. 2.6°C	-	-
14	Islande : 66.5°N, 19.5°W et 66.55°N, 17.68°W Norvège : 60.85°N, 3.72°E et 60.87°N, 3.73°E Écosse : 56.67°N, 5.83°W	Eiriksson <i>et al.</i> , 2006	Islande, Norvège, Écosse	2000-0	Islande : moins de 20 ans Norvège : 4 à 22 ans Écosse : 7 ans	Islande : isotopes stables, diatomées, analyses sédimentologiques, diptolyses Norvège : isotopes stables Écosse : isotopes stables	Islande : débris glaciaires (vélage), température de surface de l'océan Norvège : changements de température dans le flux du courant Nord Atlantique Écosse : température des eaux de fond en Été	Écosse : oscillations décennales à centennales	Islande : 2°C Norvège : 2°C Écosse : 1 à 2°C	650-50	Islande : 1050-850

Tableau de synthèse des enregistrements paléoclimatiques de l'Holocène dans le domaine océanique (voir Figure précédente pour la carte de localisation)

Numéro associé à la carte de localisation	Coordonnées	Auteurs	Site/région d'étude	Intervalle de temps étudié (année)	Résolution temporelle	Proxies utilisés	Paramètres étudiés	Périodicité(s) des événements	Amplitude des événements	Petit Âge Glaciaire (cal. BP)	Période Chaude Médievale (cal. BP)
15	69.48°N, 18.38°E	Husum <i>et al.</i> , 2004	Norvège (Malangenfjord)	8000-1600	33 à 78 ans	Foraminifères benthiques et isotopes stables	Températures des eaux de fond	Oscillations millénaires	3°C	—	—
16	68.3°N, 29.91°W	Jennings <i>et al.</i> , 1996	Groenland (Narsen Fjord)	1300-0	4 à 9 ans	Foraminifères benthiques et planctoniques, lithofaciès, analyses sédimentologiques	Débris glaciaires (vélage), glace de mer, masses d'eau régionales	—	—	320-45	1220-840
17	66.5°N, 19.07°W	Jiang <i>et al.</i> , 2002	Islande	4600-0	—	Diatomées	Température de surface de l'océan en été	—	1-2°C	Centré à 350	Centré à 850
18	62.36°N, 6.16°E	Mikalsen <i>et al.</i> , 2001	Norvège (Sulaifjord)	5500-0	17 à 22 ans	Foraminifères benthiques et $\delta^{18}O$	Oxygénation et température des eaux de fond	—	Min 2°C	325	—
19	66.96°N, 7.63°E	Risebrobakken <i>et al.</i> , 2003	Mer de Norvège (Plateau de Voring)	13 800-0	15 à 27 ans	$\delta^{18}O$ des foraminifères	Température de surface de l'océan	Faibles périodicités décennales, centennales et millénaires (1400, 1250, 1150, 900, 570, 550, 417, 260, 115, 81 ans)	2°C	—	—
20	66.55°N, 17.68°W	Rousse <i>et al.</i> , 2006	Islande	10 000-0	10 à 20 ans	Analyses paléomagnétiques	Transport du sédiment et taille des grains	Oscillations centennales (714, 238, 167, 104 ans)	—	620-150	930-620
21	75°N, 14°E	Sarnthein <i>et al.</i> , 2003	Mer de Barents	14 000-700	10 à 70 ans	Foraminifères planctoniques	Température de surface de l'océan	1000-1350, 885/840, 400-650, 505/605, 230, 145 et 92/95 ans	< 4°C	—	—
22	50.2°N, 45.68°W et 58.2°N, 48.37°W	Solignac <i>et al.</i> , 2004	Islande	8000-2500	100 à 300 ans	Dinokystes	Température et salinité de surface de l'océan, couvert de glace de mer	Oscillations millénaires	Max. 5°C	—	—

CHAPITRE I

VARIABILITY OF SEA-SURFACE TEMPERATURE AND SEA-ICE COVER IN THE FRAM STRAIT OVER THE LAST TWO MILLENNIA

Sophie Bonnet^{1,*}, Anne de Vernal^{1,*}, Claude Hillaire-Marcel¹, Taoufik Radi¹,
Robert F. Spielhagen^{2,3}, Katrine Husum⁴ and Morten Hald⁴

¹ Centre de recherche en géochimie isotopique et en géochronologie (GEOTOP),
Université du Québec à Montréal, Case postale 8888, Succursale Centre-Ville, Montréal,
Québec, Canada, H3C 3P8. Tel: +1-514-987-4080; Fax: +1-514-987-3635

² Academy of Sciences and Literature Mainz, Geschwister-Scholl-Str. 2, D-55131,
Mainz, Germany

³ Leibniz Institute for Marine Sciences, East Coast Building, Wischhofstr. 1-3,
D-24148, Kiel, Germany

⁴ Department of Geology, University of Tromsø, Dramsveien 201, N-9037 Tromsø,
Norway

*Corresponding authors: E-mail: s.bonnet@wanadoo.fr ; deveral.anne@uqam.ca

Abstract

A sediment core located on the West Spitzbergen margin in the Fram Strait (78.92°N 6.77°E, water depth: 1497 m) was analyzed for its dinocyst content in order to reconstruct hydroclimatic variations of the last 2500 years. The relative abundance of dinocyst taxa and principal component analysis show a major transition at about 300 cal. years BP. It is characterized by the disappearance of thermophilic taxa *Spiniferites mirabilis-hyperacanthus* and *Impagidinium sphaericum* and the increase of polar-subpolar taxa *Impagidinium pallidum* and *Pentapharsodinium dalei*. Sea-surface temperature (SST) estimates suggest warmer conditions than present (anomaly $\sim +2^{\circ}\text{C}$) averaging at 7°C in summer until 300 cal. years BP, although cooling pulses are recorded around 1700, 1500, 1200 and 800 cal. years BP. The last 300 years were marked by a cooling trend from 7.6 to 3.5°C and sea-ice cover up to 7 months/yr. The results demonstrate that the Fram Strait area is sensitive to hydroclimatic variations, notably with respect to sea-ice and SSTs, which are linked to the relative strength of northward flow of North Atlantic waters to the East and southward outflow of cold and fresh waters from the Arctic Ocean. Based on our data, the thermal optimum recorded around 1320 cal. years BP is the only interval of the last 2500 years that provides a possible analogue for the modern post-AD 2000 interval, which is characterized by sea-ice free conditions.

Keywords: Holocene, Nordic Seas, Fram Strait, sea-surface conditions, dinocyst

1. Introduction

Located North of the Greenland Sea, the Fram Strait is the major gateway between the Arctic and North Atlantic oceans (Figure 1). It is a key area with respect to poleward heat transport through the North Atlantic Current (NAC) to the East and freshwater fluxes from the Arctic to the North Atlantic to the West. Whereas the NAC inflow represents 35 Sv (Krauss et al., 1987), the total freshwater outflow is estimated around 160 mSv (80 mSv as ice and 65-95 mSv as liquid) according to Dickson et al. (2007). Thus, exchanges taking place in the Fram Strait play an important role in polar climate, sea-ice cover extent and thermohaline properties of upper water masses in the Nordic Seas. At high latitudes of the Northern Hemisphere, numerous studies have shown instabilities in the Holocene climate. They include studies on Greenland ice cores (e.g., O'Brien et al., 1995; Alley et al., 1997), speleothems (e.g., McDermott et al., 2001), tree-rings (e.g., MacDonald et al., 2000; Bennike, 2004) and marine cores (e.g., Bond et al., 1997; Campbell et al., 1998; Bianchi and McCave, 1999; Husum and Hald, 2004). In particular, some studies led by Hald et al. (2004, 2007) and Ślubowska-Woldengen et al. (2007) in the area of Svalbard show a gradual cooling from 8800 cal. years BP to the late Holocene, possibly resulting from regional decrease in the contribution of Atlantic water fluxes to polar waters. However, due to low sedimentation rates in marine environments, paleoceanographic reconstructions often lack of temporal resolution to document decadal to centennial timescale variations of the late Holocene (e.g., Hald et al., 2004).

Here, our objective is to develop a high-resolution record of ocean and climate variations during the late Holocene in the Fram Strait based on the analysis of core JM-06-WP-04-MCB (JM04 in the text; 78.92°N 6.77°E, water depth: 1497 m; Figure 1), which is located on the slope of the western continental margin of Svalbard, in an area characterized by relatively thick Holocene sedimentary sequence (Husum, 2006). In the present study, we report on the paleoclimate record of core JM04 based on

organic-walled dinoflagellate cysts (or dinocysts), which permit the reconstruction of sea-surface conditions, including winter and summer sea-surface temperatures (SSTs), salinities (SSSs) and sea-ice cover (de Vernal et al., 1994, 1997, 2001, 2005; de Vernal and Marret, 2007). In subpolar environments, dinocysts are usually well preserved in sediments and distribution of their assemblages is closely related to hydrographical parameters, notably to the seasonal sea-ice extent.

In order to better understand the distribution of dinocyst assemblages in the Nordic Seas and Fram Strait prior to making quantitative reconstructions at the coring site, we have developed a regional dataset with surface sediment samples collected during WarmPast expeditions JM-06-WP and JM-07-WP (Figure 2) (Husum, 2006, 2007). The regional dataset that comprises 94 sites North of 70°N was used for multivariate analyses with the aim to define the relationships between dinocyst assemblages and hydrographic conditions with the best possible accuracy (Figure 2). It was combined with the North Atlantic and Arctic dinocyst database (de Vernal et al., 2005) for the reconstructions of sea-ice cover, sea-surface temperatures and salinity using the modern analogue and artificial neural network techniques (e.g., Guiot and de Vernal, 2007).

2. Modern oceanic setting

The surface currents in the Fram Strait are characterized by two main components: (1) the Arctic sea-ice and freshwater discharge flowing southward along the Greenland margin and forming the East Greenland Current (EGC); (2) the North Atlantic current (NAC) to the East which mixes with the East Spitsbergen Current (ESC) and forms the West Spitzbergen Current (WSC) flowing northward into the Arctic Ocean (Dickson et al., 2007; Walczowski et al., 2005) (Figure 1). The WSC arises from the North Atlantic Drift (NAD) and constitutes its northernmost extension. The NAD water mass is warm and saline, becoming colder and fresher toward high latitudes, with SSSs and SSTs gradients ranging from 35.45 to 35.04 and

10.5°C to 3.1°C between the Greenland-Scotland Ridge (57° to 66°N) and Fram Strait (75°N) (Hansen and Østerhus, 2000; Walczowski et al., 2005). In winter, the cooling of North Atlantic waters in the Nordic Seas is accompanied by convection, thus playing a major role in the formation of the North Atlantic Deep Water (NADW) and thermohaline circulation (Hansen and Østerhus, 2000; Rudels et al., 2005; Dickson et al., 2007; Komuro and Hasumi, 2007). Surface waters at the location of core JM04 are principally influenced by the WSC. Studies led by Fahrbach et al. (2001) between September 1997 and August 1999 indicate a mean transport at 78°50'N of 9.5 ± 1.4 Sv northward (through the WSC) and 11.1 ± 1.7 Sv southward (through the EGC) at 79°N. The balance of northward flow takes place in the Barents Sea (e.g., Schauer et al., 2002). The EGC carries fresher and colder waters with a total freshwater flux (ice and liquid) of roughly 160 mSv (80 mSv as ice and 65-95 mSv as freshwater) (Dickson et al., 2007; Holfort and Meincke, 2005).

At the coring site, mean modern SSTs (1930-2001) are $-0.13 \pm 1.27^\circ\text{C}$ in February and $5.17 \pm 1.62^\circ\text{C}$ in August. Modern SSSs are 34.79 ± 0.12 in February and 34.31 ± 0.78 in August (NODC, 2001). The large standard deviations of temperatures and summer salinity indicate high interannual variability of sea-surface conditions in this area. It can be explained by the site location close to the Arctic Front that separates the Atlantic and Arctic water masses and corresponds to the maximum limit of sea-ice in winter (Figure 1). Figure 3a represents the 1953-2001 sea-ice data (concentration greater than 50%) provided by the National Snow and Ice Data Center (NSIDC, <http://nsidc.org/index.html>) and historical records (concentration greater than 30%) from the Arctic Climate System Study (ACSYS, 2003). Both data sets show large amplitude variations of seasonal coverage from one year to another, with sea-ice ranging from 0 to 6 months/yr. Since 1982, no sea-ice cover was recorded around the site, which is probably a regional consequence of the post-industrial warming (IPCC, 2007). Sea-ice variations in Fram Strait seem interrelated with surface air temperature, which also record large amplitude

variations, especially in winter (Figure 3b). These data are available at: <http://www.ipcc-data.org/index.html>.

3. Material and methods

The samples analyzed were collected with a multi-corer (MC) or box corer (BC) during the expeditions of R/V *Jan Mayen* (Husum, 2006, 2007) and the *Healy-Oden Trans Arctic Expedition* (HOTRAX; Darby, 2005). The multi-core JM04 is 54 cm long and was sub-sampled at 1 cm interval. Surface sediment (0-1 cm) samples from all other cores were sub-sampled and used to improve the reference database (Table 1).

In the upper 3 cm of core JM04, ^{210}Pb , ^{137}Cs measurements were performed in order to identify the depth of biological mixing and to evaluate the sediment accumulation rate. Five AMS- ^{14}C measurements on planktic foraminifera (*Neogloboquadrina pachyderma* and *Globigerina bulloides*) allowed the establishment of a chronology (Figure 8 and Table 2). The software Calib 5.0.2 (Stuiver et al., 2000) was used for calibration after correction for a 400-year atmosphere-ocean reservoir difference and normalization for a $\delta^{13}\text{C}$ of -25‰ PDB (MARINE04 calibration curve) (Hughen et al., 2004). All ages are reported as calibrated years BP (AD 1950 = 0 cal. years BP).

Samples were processed using standard palynological procedure (de Vernal et al., 1996). About 5 cm³ of sediments were sieved on 106 μm and 10 μm mesh sieves to eliminate the coarse and fine fractions. The fraction between 10 and 106 μm was treated 4 times with warm HCl (10%) and 3 times with warm HF (49%) to dissolve, respectively, carbonate and silica particles. The remaining residue was mounted between slide and cover-slide in glycerin gel for observation in transmitted light microscopy at 400x magnification. A minimum of 250 dinocyst specimens were counted and identified in each sample. Pollen grains, spores and organic linings of benthic foraminifera were also counted. Only dinocyst results are presented here and

the detailed palynological results are reported in Bonnet (2009). Dinocyst taxa were identified using the nomenclature in Rochon et al. (1999) and Head et al. (2001). Concentration of palynomorphs was calculated from the marker-grain method (Matthews, 1969), which provides results with an accuracy of about 10% for a 0.95 confidence interval (de Vernal et al., 1987).

Modern hydrographic data at surface sample sites were compiled from databases of NODC (2001) and NSIDC (2003). Compilations of SSTs and SSSs were made from measurements performed between AD 1930-2001 within a radius of 30 nautical miles around sites. Sea-ice data were compiled for the interval between 1953 and 2001 within a grid of 1 degree by 1 degree of latitude and longitude. Sea-ice is expressed as the number of months per year with a concentration greater than 50%. Data from ACSYS are interpreted from ice edge position, i.e., they are defined by a set of geographic coordinates, which are compiled using polylines and polygons in GIS files. Data from the period 1553-2002 are assembled in ACSYS historical ice chart archives provided by the Norwegian Polar Institute (ACSYS, 2003). For periods with scattered data, interpolations were applied for months with no available data. It concerns mainly wintertime prior to 1750. Until 1966, data were derived from aircraft observations, ship logbooks, diaries, newspaper reports and maps. From 1966 to 2002, data constitute a combination of satellite imagery and in situ observations.

Principal component analysis (PCA) and canonical correspondence analysis (CCA) were performed with the software XLSTAT (Addinsoft, 2008). CCA was performed on the 94 surface samples of the Nordic Seas, between 70°N and 80°N and 20°W to 20°E (Figure 2) and PCA was applied on core JM04 assemblages.

Reconstructions of past sea-surface conditions were made using two different approaches for comparison and to insure the robustness of estimates. We used the modern analogue technique (MAT), which is based on the similarity degree between fossil and modern spectra and assumes fossil assemblages developed in environmental conditions that are similar to their modern analogues (Guiot, 1990).

We also used the artificial neural network (ANN) technique, which relies on calibration between hydrographical parameters and assemblages (cf. Malmgren and Nordlund, 1997). Among transfer function methods currently used in paleoceanography, MAT and ANN perform the best although both have caveats (e.g., Kucera et al., 2005; Guiot and de Vernal, 2007).

Reconstructions from MAT were made using the Northern Hemisphere reference database that includes 1189 sites in addition to the 19 surface samples from the Fram Strait analyzed here (Figure 4). We followed the procedures described by de Vernal et al. (2005) and we used a set of ten analogues for estimating past sea-surface conditions. Reconstructions from ANN were based on two different calibration data sets following the procedures described by Peyron and de Vernal (2001). The geographical domain of the calibration data set is important since it may introduce a bias in reconstructions with equivalent error of prediction as shown by Peyron and de Vernal (2001). One calibration data set comprises all sites from the North Atlantic and Arctic oceans, including adjacent seas ($n = 735$). The other calibration data set was constrained on the basis of the geographical domain determined from the location of analogues in core JM04 ($n = 437$; Figure 4). MAT and ANN were performed using the R software, available at this website: <http://www.r-project.org/>, with scripts adapted by Guiot from PPPbase (Guiot and Goeury, 1996; <http://www.imep-cnrs.com/pages/3pbase.htm>).

Quantitative reconstructions of winter and summer SSTs, summer SSSs and seasonal sea-ice cover ($> 50\%$) duration in months/year were performed. Validation tests of MAT and ANN with the two calibration data sets were made in order to evaluate the respective performance of each approach and to calculate the error of prediction (Table 3). The reliability of approaches is given by the coefficient of correlation (R^2) between observed and estimated values, whereas the accuracy is provided by the root mean square error (RMSE) that corresponds to the standard deviation of the difference between observed and estimated values. The root mean

square error of prediction (RMSEP) is calculated by dividing the database in calibration (5/6) and verification data sets (1/6) (Guiot and de Vernal, 2007). The use of verification data set, which represents 1/6 of the database for the RMSEP calculations, avoids the problem of spatial autocorrelation (Telford, 2006). On the whole, all approaches provide good results, the best ones being obtained with MAT (Table 3).

4. Results

4.1. Dinocyst assemblages in surface sediments from the Nordic Seas

Surface sediment samples collected in 2006 and 2007 in the Fram Strait contain abundant dinocysts, with concentrations ranging from 195 cysts/cm³ along the Greenland margins to 28 000 cysts/cm³ in eastern Fram Strait (Figure 5). The dinocyst assemblages are dominated by the ubiquitous taxa *Operculodinium centrocarpum* and *Nematosphaeropsis labyrinthus*, in addition to *Islandinium minutum* and *Brigantedinium* spp., which often dominate in Arctic seas (e.g., Rochon et al., 1999; de Vernal et al., 2001; Matthiessen, 1995). Accompanying taxa include *Impagidinium pallidum*, *Spiniferites elongatus*, *Spiniferites ramosus* and *Pentapharsodinium dalei* (Figure 5).

I. minutum and *Brigantedinium* spp. occur principally along the eastern Greenland margin as documented by Rochon et al. (1999) (Figure 5). *I. pallidum* is mostly abundant in the open ocean settings and *P. dalei* is common in most samples. *S. ramosus* and *S. elongatus* are frequent in low numbers as accompanying taxa.

CCA analyses were performed on the assemblages from the 94 sites of the Nordic Seas (Figure 6). Axis 1 (CCA 1) represents 77.27% of the total variance. It is defined by negative scores of *I. minutum* and *Brigantedinium* spp., which belong to Protoperidinales, and are generally associated with heterotrophic productivity. Axis 1 is also defined by positive scores of all other taxa, which can be mostly associated with phototrophic behavior (e.g., Taylor and Pollinger, 1987). Axis 1 correlates

negatively with sea-ice cover ($R^2 = -0.989$) and positively with August SSTs ($R^2 = 0.939$) and SSSs ($R^2 = 0.909$) (Figure 6). The geographical distribution of CCA axis 1 illustrates a strong relationship between dinocyst assemblages and sea-ice cover, positive values being associated with ice-free areas that are predominantly influenced by the North Atlantic Current. Conversely, negative values of CCA axis 1 correspond to the sites characterized by extensive sea-ice cover along the margins of the eastern Greenland coast marked by outflow of Arctic waters (Figure 7). CCA axis 2 explains 12.81% of the variance. It shows an opposition between *I. pallidum* and *N. labyrinthus* on one side, and the other taxa on the other side (Figure 6). Geographical distribution of axis 2 scores shows that the most negative values occur in the central part of the Nordic Seas, whereas positive values correspond to neritic regions (Figure 7).

4.2. Core JM04

4.2.1. Chronology

The age vs. depth relationship in the core has been established from AMS- ^{14}C measurements on planktonic foraminiferal populations and ^{210}Pb measurements in core-top sediments (Table 2, Figure 8). A first order estimate of sedimentation rates has been obtained from a linear regression using the calibrated ^{14}C -ages between 11.5 and 48.5 cm. It indicates a mean sedimentation rate of about 18 cm/kyr and suggests a core-bottom age of 2500 years. However, the spreading of datum points around the regression line ($R^2 = 0.99$) points to relatively variable sedimentation rates. This is further indicated by core-top ^{210}Pb and ^{137}Cs data.

Nearly constant ^{210}Pb activities down to approximately 3 cm lead to set a mixed-layer boundary at this depth, but with incomplete mixing through bioturbation, as suggested by ^{137}Cs activities peaking some 1.5 cm below core top (Figure 8a). Below 3 cm and down to 8 cm, $\ln^{210}\text{Pb}$ -excesses show a decreasing linear trend leading to estimate a mean sedimentation rate of 94 cm/kyr. Extrapolating this rate up

to the core top, the age of the 3 cm-thick mixed layer can be estimated using the equation below (cf. Berger and Johnson, 1978):

$$T = 1/\lambda \times \ln[1 + (\lambda x/S)]$$

where λ is the decay constant, x is the mixed-layer thickness, S the sedimentation rate and T , the radiometric age of the mixed layer. A “ T ” value of about 30 years is obtained here.

A significant decline in the ^{210}Pb -excess (from 12 to 1.3 dpm/g) is seen between mid-sample depths of 7.5 and 8.5 cm, suggesting a major drop in sedimentation rate. A poorly constrained value of about 18 cm/kyr can be calculated, contrasting sharply with the value estimated for the overlying sediment (94 cm/kyr). Nonetheless, the calibrated ^{14}C -age of 213.5 ± 40.5 years yielded by foraminifers at a depth of 11.5 cm and the mean sedimentation rate estimated above for the 11.5 and 48.5 cm section fit with this scenario, as illustrated in Figure 8b.

The cause of a sharp rise in the sedimentation rate dating from approximately a century ago is unknown but we observe changes in grain size, which indicate variations in detrital inputs (Figure 8c). The upper part of the sequence is marked by an increased proportion of coarse sand (fraction $>106 \mu\text{m}$) and probably corresponds to higher sedimentary supply, notably through ice rafting. The significant decrease in dinocyst concentrations in the upper few centimeters of the core could also be explained by higher sedimentation rates and dilution with higher sedimentary inputs (cf. Figure 9b).

The final age model used for this core is based on a mixed layer age around 30 years, followed by a 90-year interval with high sedimentation rate, then ages interpolated from ^{14}C -data assuming unchanged reservoir correction of 400 years for each datum before calibration. It is worth mentioning that assuming a constant 3 cm-thick mixed layer, bioturbation mixing would limit the temporal resolution to about 30 years near core top to approximately 150 years below.

4.2.2. Dinocyst record

Dinocysts are abundant in all samples from core JM04 with concentrations ranging from 4000 to 38 000 cysts/cm³. This corresponds to fluxes ranging from 376 to 684 cysts/cm²/yr (Figure 9b). Such values are characteristic of high productivity continental margin environments (e.g., de Vernal et al., 1994).

Dinocyst assemblages of core JM04 (Figure 9) are dominated by *O. centrocarpum* (60-90%), with abundant *I. minutum* (0.4-22%), *N. labyrinthus* (1-13%) and *Brigantedinium* spp. (0.1-11%). Accompanying taxa include *S. elongatus*, *S. ramosus*, *P. dalei* and *I. pallidum*. In the lower part of the sequence, assemblages also include thermophilic taxa, which occur rarely in surface sediment samples of the Nordic Seas. These taxa are *Spiniferites mirabilis-hyperacanthus*, *Selenopemphix quanta* and *Impagidinium sphaericum* (Figures 9 and 11).

We performed a PCA on taxa percentages (Figure 10). The first principal component (PC 1) explains 27.65% of the total variance and shows an opposition between *I. pallidum*, *S. ramosus*, *P. dalei* and *I. minutum* on one side and *I. sphaericum*, *S. mirabilis-hyperacanthus* and *O. centrocarpum* on the other side. Thus, PC 1 seems to reflect an opposition between polar-subpolar taxa and more thermophilic ones. The second principal component (PC 2) represents 16.48% of the variance and shows an opposition between *I. minutum*, *Brigantedinium* spp. and *S. quanta* on one side and most other taxa on the other side. PC 2 therefore seems to be determined by the trophic behavior of taxa (i.e. heterotrophic vs. phototrophic).

On the basis of taxa percentages and PCA, we can distinguish two assemblage zones (Figures 9-10). The lower zone, spanning 2500 to 300 cal. years BP is characterized by positive values of PC 1, with the occurrence of *S. mirabilis-hyperacanthus*, *S. quanta*, and *I. sphaericum*. It suggests relatively mild sea-surface conditions. The upper zone, covering from 300 cal. years BP to present, is marked by negative PC 1, the absence or rarity of thermophilic taxa *S. mirabilis-hyperacanthus*, *S. quanta* and *I. sphaericum*, and relatively high percentages of *I. pallidum*. This zone

is also characterized by increased percentages of *I. minutum*. On the whole, the upper zone reflects colder conditions than the lower one.

4.2.3. *Quantitative reconstructions of sea-surface conditions*

Sea-surface conditions were reconstructed quantitatively from dinocyst assemblages using MAT and ANN as briefly described in the material and methods section (Figure 12). Validation tests suggest that MAT provides the most accurate results (Table 3), but ANN was nonetheless used as a means to verify the robustness of the estimates and trends. It is worth to mention the RMSEP is lower than the RMSE for most parameters using the MAT. This demonstrates that spatial autocorrelation does not bias the MAT results (Telford, 2006).

The MAT applied to assemblages of core JM04 shows that most modern analogues are located in the Nordic Seas and northern North Atlantic (Figure 4b). It also shows that good analogues with high degree of similarity exist for all assemblages of core JM04, with distance considerably below the threshold value for poor analogue situation (Table 4). Therefore, given the high dinocyst concentrations in samples suggesting a high regional production, the accuracy of the approach as defined from validation exercises and the degree of similarity of selected analogues, MAT results meet all reliability criteria (de Vernal et al., 2005; Kucera et al., 2005; Guiot and de Vernal, 2007).

Results from ANN are generally consistent with those obtained from MAT, especially for summer and winter temperatures. Time series from ANN, however, show a lesser variability and amplitude of changes than those from MAT, which suggests a smoothing effect from calibrations. Nevertheless, the SST curves are nearly identical and show oscillations between -1°C and 5.5°C in winter and between 2.4°C and 10.0°C in summer. From 2500 to 300 cal. years BP, SSTs were relatively high with mean values of about 2°C and 7°C in winter and summer, respectively. Warm phases are recorded around 1900, 1600, 1320, 1120 and 325 cal. years BP,

with an optimum centered at 1320 cal. years BP. After 300 cal. years BP, SSTs were significantly lower with mean values of about 0°C and 3.5-4°C in winter and summer, respectively.

Salinity reconstructions show discrepancies, not only between MAT and ANN, but mostly between ANN reconstructions based on the two different calibration databases. By applying the North Atlantic-Arctic database that includes a wide range of salinity (from 20 to 36), the reconstructed summer salinity with ANN is relatively low (mean of 33). Conversely, by using the North Atlantic database as delimited by the distribution of analogues in core JM04 (Figure 4b), the reconstructed salinity with ANN is relatively high (mean of 34). The MAT estimates average around 33.5 and vary between the maximum and minimum values provided by ANN estimates. It thus seems the ANN estimates are biased toward low and high salinity depending upon the calibration database. Salinity reconstructions from MAT seem more reliable and suggest high salinity variability, ranging from 30.5 to 35. Of interest here, are the low salinity peaks recorded around 2240, 640 cal. years BP and at the top of the sequence (280 cal. years BP). They correspond to cool phases and suggest important outflow of low saline Arctic water. The maximum salinity recorded at about 1320 cal. years BP corresponds to the thermal optimum and underlines maximum northward flow of warm and saline North Atlantic Current in the eastern Fram Strait.

Sea-ice estimates based on MAT and the two ANN calibrations also show discrepancies. In general, estimates from MAT yield higher sea-ice values than ANN, and ANN calibration using the North Atlantic data alone yields the lowest values. Here again, ANN reconstructions appear biased depending on the calibration database chosen. Given the lower sea ice RMSEP from MAT (Table 3), we are more confident with MAT results. Moreover, the MAT estimates of sea-ice cover during the last centuries are in agreement with historical data (see Figure 3), in contrary to ANN estimates. In any case, despite some uncertainties, there are consistent features in the sea-ice record, notably the existence of ice-free conditions during the thermal

optimum centered at about 1320 cal. years BP and the increased trend of sea-ice cover after 300 cal. years BP, with maximum values up to 7 months/yr in a sub-recent interval. Moreover, all approaches lead to reconstructions showing the spreading of sea-ice cover during the cooling pulses recorded around 1700, 1500 and centered to 800 cal. years BP.

5. Discussion

Reconstructions of sea-surface conditions were performed in core JM04 that spans the last 2500 years. According to the age model based on ^{210}Pb and ^{14}C measurements, sedimentation rates average around 18 cm/kyr throughout most of the sequence and reach up to 94 cm/kyr in the upper part of the core (0-8 cm), representing the last century. Taking into account mixing by bioturbation over 3 cm thick layers, the time resolution achieved with analyses performed at one cm interval is about 160 years for the interval spanning 2500 to 100 cal. years BP. Such a chronological resolution is not as high as expected, but it nevertheless remains the best one available for late Holocene marine records in the northern part of the Nordic Seas. The paleoceanographical time series of core JM04 we established, based on dinocyst assemblages, is also unique since it allows documenting sea-surface salinity and sea-ice cover in addition to sea-surface temperature.

Beyond uncertainties inherent to the application of transfer functions (see sections 3 and 4.2.3 and Table 3) and despite the smoothing effect of bioturbation, the results demonstrate large amplitude variations of temperatures, from 2 to 10°C in summer, and from -1 to 5.5°C in winter. They also show large amplitude changes in sea-ice, from ice-free conditions up to 7 months/yr, and summer salinity variations from 30.7 to 34.9. Clearly, the area of the Fram Strait is extremely sensitive to climate and ocean changes as also shown from the historical sea-ice records (Figure 3) and hydrographic data (NODC, 2001).

Numerous studies in high latitudes of the North Atlantic Ocean and surrounding lands led to document climate changes during the Holocene with amplitude ranging from 1 to 3°C (e.g., Bendle and Rosell-Melé, 2007; Ślubowska-Woldengen et al., 2007; Hald et al., 2004, 2007; Rousse et al., 2006; Eiriksson et al., 2006; Solignac et al., 2004; Husum and Hald, 2004). At the scale of the last two millennia, most data come from Scandinavia, Greenland, Svalbard and Iceland, and there are a few records available from the marine realm (e.g., compilation in IPCC, 2007). In most of records, the largest climate change is associated with the transition from the Medieval Warm Period (MWP) to Little Ice Age (LIA). For example, data from the Vøring Plateau suggest a cooling of ~2°C at 600-500 cal. years BP based on stable isotopes and planktic foraminifers (Andersson et al., 2003). As another example, alkenone and diatom data from the North Icelandic Basin area permitted to reconstruct a cooling of about 1-2°C around 350 cal. years (cf. Bendle and Rosell-Melé, 2007; Jiang et al., 2002). Among the terrestrial records, those from Scandinavia and Ireland suggest that the LIA cooling was 2°C in amplitude and began around 800 cal. years BP (Seppä et al., 2002; Nesje et al., 2001; Karlén and Kuylénstierna, 1996). As illustrated from the examples above, there are many proxy data documenting climate changes related to the transition from the MWP to the LIA, but the amplitude and timing of the LIA cooling remains equivocal. The discrepancies from one record to another may reflect regionalism in the climate change. They may also result from uncertainties in age models and from different sensitivity of the proxies. The reconstructions from core JM04 illustrate higher amplitudes of temperature changes (up to 5°C) than what is reported in the literature, which can be related to higher sensitivity of the dinocyst proxy as compared to others in a subpolar-polar context (e.g., Solignac, 2004; de Vernal et al., 2005, 2006) or to the location of the coring site close to the Arctic Front, probably to both.

In the core JM04, dinocyst assemblages led to identify a thermal optimum dated from 1450 to 1300 cal. years BP. This optimum is marked by sea-ice free conditions,

SSTs reaching 5°C in winter and 10°C in summer and salinity slightly above the modern value. It is the only interval of the JM04 record showing conditions as warm as the ones observed since the late eighties (Figure 3). The 1450-1250 cal. years BP optimum corresponds probably to maximum strength of the NAC, which resulted in a northward shift of the Arctic Front. At the scale the northern North Atlantic region, this interval is not identified as a thermal optimum. On the contrary, it rather corresponds to a cooling in the Rockall and Vøring Plateau areas (Bond et al., 1997; Andersson et al., 2003). If we assume the chronology is correct, the discrepancies between the Fram Strait record and those of the Rockall and Vøring Plateau could reflect regionalism in the strength and characteristics of the eastern and western branches of the North Atlantic Current in the northern North Atlantic.

The record of sea-surface conditions from core JM04 indicates warmer than modern winter SSTs during the last 2500 years. The only exception is the interval spanning from 250 to 50 years BP, which is characterized by particularly low temperatures both in winter and summer. This interval illustrates a major change in dinocyst assemblages with the disappearance of *Selenopemphix quanta* and *Spiniferites mirabilis-hyperacanthus*. It also corresponds to an interval of abundant ice-rafted debris. A cold event dated at about 350-300 cal. years BP has been recorded in a few sequences, notably North of Iceland (Jiang et al., 2002; Bendle et al., 2007), off eastern Greenland (Jennings et al., 1996) and along the western Norwegian coast (Mikalsen et al., 2001). This event is commonly associated with the latest phase of the LIA. Although apparently younger, the drastic cooling recorded in core JM04 is probably correlative taking into account the chronological uncertainties.

Beyond temperature and sea-ice fluctuations, our reconstructions point out two major low salinity events, down to 31, at about 2340 and 700 cal. years BP. These events indicate dilution with freshwater outflow from the Arctic. It is worth mentioning that the freshwater event dated between 850 and 550 cal. years BP corresponds to the onset of the LIA in many marine and terrestrial paleoclimate

records of the circum Atlantic region (Nesje et al., 2001; Seppä et al., 2002; Andersson et al., 2003; Eriksson et al., 2006; Rousse et al., 2006). This supports the hypothesis of thermohaline circulation weakening as a cause of the LIA.

6. Conclusion

Dinocyst assemblages of surface sediment samples in the Fram Strait and Nordic Seas show a geographical distribution closely related to the sea-ice cover extent in addition to sea-surface temperature and salinity. It relates to the main path of surface circulation, the EGC exporting fresh and cold water from the Arctic to the West and the WSC bringing water masses warmer and saltier from the North Atlantic to the East. Thus, in the context of the Fram Strait, dinocysts are a suitable proxy for paleoceanographical conditions, especially since they are well preserved and form assemblages characterized by relatively high diversity of species. The analyses of core JM04 in the eastern Fram Strait show that important changes of sea-surface conditions occurred during the last 2500 years. In general, the late Holocene is characterized by SSTs warmer than present, but centennial oscillations of winter and summer temperatures and sea-ice cover indicate the limit of the Arctic Front remained close to the coring site throughout most of the last two millennia. From 1450 to 1300 cal. years BP, particular warm (up to 5.5°C in summer) and saline (> 34 in summer) water masses characterized the area together with year-round ice-free conditions. This corresponds to the only interval during which the Arctic Front shifted significantly to the north in Fram Strait due to poleward penetration of warm and saline North Atlantic Waters at the surface before subducting into the Arctic Ocean. In contrary, from 250 cal. years BP to the upper part of the sequence, particularly harsh conditions are recorded with sea-ice cover reaching up to 7 months/yr. Such a cooling event might constitute the regional signature of the LIA, but would correspond to its later phase. Beyond these paleotemperature peaks and centennial oscillations of SSTs, the record shows large amplitude variations of

salinity with minimum values (< 33 in summer) between 850 and 550 cal. years BP. This interval coincides with the LIA as recorded at many middle-high latitude sites of the Northern Hemisphere (e.g., IPCC, 2007). This low salinity episode in the Fram Strait probably corresponds to freshwater outflows from the Arctic and might be at the origin of lower density in surface water of the Nordic Seas, thus reduced strength of the deep-water formation and thermohaline circulation in the northern North Atlantic. From this point of view, the record of core JM04 points to instabilities that are related to the dynamic of freshwater fluxes from the Arctic to the North Atlantic. This study demonstrates the sensitivity of the Fram Strait area, suggests variations in the strength and/or the latitude reached by the NAC as well as fluctuations in the thermohaline circulation.

7. Acknowledgements

This study is a contribution to the Polar Climate Stability Network (PCSN) supported by the Canadian Foundation for Climate and Atmospheric Sciences (CFCAS). Additional support was provided by the *Fonds Québécois de la Recherche sur la Nature et les Technologies* (FQRNT) and the Natural Sciences and Engineering Research Council of Canada (NSERC). It is also a contribution to the WARMPAST (Arctic Ocean Warming in the Past) project in the context of the International Polar Year (IPY n°36) supported by the University of Tromsø and the Research Council of Norway. Thanks are also due to Maryse Henry (GEOTOP) for her help in the laboratory and to Bassam Ghaleb (GEOTOP) for Lead-210 and Cesium-137 measurements.

8. References

- ACSYS, 2003. ACSYS Historical Ice Chart Archive (1553-2002), IACPO Informal Report 8. Digital Media, Arctic Climate System Study, Norwegian Polar Institute, Tromsø, Norway.
- Addinsoft, 2008. XLSTAT 2008, Data Analysis and Statistics Software for Microsoft Excel. Paris, France.
- Alley, R.B., Mayewski, P.A., Sowers, T., Stuiver, M., Taylor, K.C. and Clark, P.U., 1997. Holocene climatic instability; a prominent, widespread event 8200 yr ago. *Geology* 25(6), 483-486.
- Andersson, C., Risebrobakken, B., Jansen, E. and Dahl, S.O., 2003. Late Holocene surface ocean conditions of the Norwegian Sea (Voring Plateau). *Paleoceanography* 18(2), PA1044. doi: 10.1029/2001PA000654.
- Bendle, J.A.P. and Rosell-Mele, A., 2007. High-resolution alkenone sea surface temperature variability on the North Icelandic Shelf: implications for Nordic Seas palaeoclimatic development during the Holocene. *The Holocene* 17(1), 9-24.
- Bennike, O., 2004. Holocene sea-ice variations in Greenland: onshore evidence. *The Holocene* 14(4), 607.
- Berger, W.H. and Johnson, R.F., 1978. On the thickness and the ^{14}C age of the mixed layer in deep-sea carbonates. *Earth and Planetary Science Letters* 41(2).
- Bianchi, G.G. and McCave, I.N., 1999. Holocene periodicity in North Atlantic climate and deep-ocean flow south of Iceland. *Nature* 397(6719), 515-517.
- Bond, G., Showers, W., Cheseby, M., Lotti, R., Almasi, P., deMenocal, P., Priore, P., Cullen, H., Hajdas, I. and Bonani, G., 1997. A Pervasive Millennial-Scale Cycle in North Atlantic Holocene and Glacial Climates. *Science* 278(5341), 1257.
- Bonnet, S., 2009. Variability of sea-surface temperature and sea-ice cover in the Fram Strait over the last two millennia M.Sc. Thesis, Université du Québec à Montréal, Montréal, Québec, Canada.

- Campbell, I.D., Campbell, C., Apps, M.J., Rutter, N.W. and Bush, A.B.G., 1998. Late Holocene approximately 1500 yr climatic periodicities and their implications. *Geology* 26(5), 471-473.
- Darby, D., 2005. CRUISE REPORT HLY0503: Healy-Oden Trans-Arctic Expedition. Department of Ocean, Earth and Atmospheric Sciences, Old Dominion University, USA.
- de Vernal, A., and Marret, F., 2007. Organic-walled dinoflagellate cysts: tracers of sea-surface conditions. In: Hillaire-Marcel, C., de Vernal, A. (Eds.), *Proxies in Late Cenozoic paleoceanography*. Developments in Marine Geology, Elsevier, pp. 371-408.
- de Vernal, A., Larouche, A. and Richard, P.J.H., 1987. Evaluation of palynomorph concentrations: do the aliquot and the marker-grain methods yield comparable results? *Pollen et spores* 29(2-3), 291-303.
- de Vernal, A., Turon, J.L. and Guiot, J., 1994. Dinoflagellate cyst distribution in high-latitude marine environments and quantitative reconstruction of sea-surface salinity, temperature, and seasonality. *Canadian Journal of Earth Sciences* 31(1), 48-62.
- de Vernal, A., Henry, M., and Bilodeau, G., 1996. Technique de préparation et d'analyse en Micropaléontologie, Les cahiers du GEOTOP 3, unpublished report, Université du Québec à Montréal, Montréal, Québec, Canada.
- de Vernal, A., Rochon, A., Turon, J.L. and Matthiessen, J., 1997. Organic-walled dinoflagellate cysts: Palynological tracers of sea-surface conditions in middle to high latitude marine environments. *Geobios(Lyon)* 30(7), 905-920.
- de Vernal, A., Henry, M., Matthiessen, J., Mudie, P.J., Rochon, A., Boessenkool, K.P., Eynaud, F., Grosfjeld, K., Guiot, J. and Hamel, D., 2001. Dinoflagellate cyst assemblages as tracers of sea-surface conditions in the northern North Atlantic, Arctic and sub-Arctic seas: the new "n= 677" data base and its application for quantitative paleoceanographic reconstruction. *Journal of Quaternary Science* 16(7), 681-698.
- de Vernal, A., Eynaud, F., Henry, M., Hillaire-Marcel, C., Londeix, L., Mangin, S., Matthiessen, J., Marret, F., Radi, T. and Rochon, A., 2005. Reconstruction of sea-surface conditions at middle to high latitudes of the Northern Hemisphere during the Last Glacial Maximum (LGM) based on dinoflagellate cyst assemblages. *Quaternary Science Reviews* 24(7-9), 897-924.

- Dickson, R., Rudels, B., Dye, S., Karcher, M., Meincke, J. and Yashayaev, I., 2007. Current estimates of freshwater flux through Arctic and subarctic seas. *Progress in Oceanography* 73(3-4), 210-230.
- Eiriksson, J., Bartels-Jonsdottir, H.B., Cage, A.G., Gudmundsdottir, E.R., Klitgaard-Kristensen, D., Marret, F., Rodrigues, T., Abrantes, F., Austin, W.E.N. and Jiang, H., 2006. Variability of the North Atlantic Current during the last 2000 years based on shelf bottom water and sea surface temperatures along an open ocean/shallow marine transect in western Europe. *The Holocene* 16(7), 1017-1029.
- Fahrbach, E., Meincke, J., Osterhus, S., Rohardt, G., Schauer, U., Tverberg, V. and Verduin, J., 2001. Direct measurements of volume transports through Fram Strait. *Polar Research* 20(2), 217-224.
- Guiot, J., 1990. Methodology of palaeoclimatic reconstruction from pollen in France. *Palaeogeography, Palaeoclimatology, Palaeoecology* 80, 49-69.
- Guiot, J. and Goeury, C., 1996. PPPBASE, a software for statistical analysis of paleoecological and paleoclimatological data. *Dendrochronologia* 14, 295-300.
- Guiot, J., and de Vernal, A., 2007. Transfer functions: methods for quantitative paleoceanography based on microfossils. In: Hillaire-Marcel, C., de Vernal, A. (Eds.), *Proxies in Late Cenozoic paleoceanography. Developments in Marine Geology*, Elsevier, pp. 523-563.
- Hald, M., Ebbesen, H., Forwick, M., Godtlielsen, F., Khomenko, L., Korsun, S., Ringstad Olsen, L. and Vorren, T.O., 2004. Holocene paleoceanography and glacial history of the West Spitsbergen area, Euro-Arctic margin. *Quaternary Science Reviews* 23(20-22), 2075-2088.
- Hald, M., Andersson, C., Ebbesen, H., Jansen, E., Klitgaard-Kristensen, D., Risebrobakken, B., Salomonsen, G.R., Sarnthein, M., Sejrup, H.P. and Telford, R.J., 2007. Variations in temperature and extent of Atlantic Water in the northern North Atlantic during the Holocene. *Quaternary Science Reviews* 26, 3423-3440.
- Hansen, B. and Østerhus, S., 2000. North Atlantic-Nordic Seas exchanges. *Progress in Oceanography* 45(2), 109-208.

- Head, M.J., Harland, R. and Matthiessen, J., 2001. Cold marine indicators of the late Quaternary: the new dinoflagellate cyst genus *Islandinium* and related morphotypes. *Journal of Quaternary Science* 16(7), 621-636.
- Holfort, J. and Meincke, J., 2005. Time series of freshwater-transport on the East Greenland Shelf at 74N. *Meteorologische Zeitschrift* 14(6), 703-710.
- Hughen, K.A., Baillie, M.G.L., Bard, E., Beck, J.W., Bertrand, C.J.H., Blackwell, P.G., Buck, C.E., Burr, G.S., Cutler, K.B. and Damon, P.E., 2004. Marine04 Marine Radiocarbon Age Calibration, 026 Cal Kyr BP. *Radiocarbon* 46(3), 1059-1086.
- Husum, K., 2006. CRUISE REPORT JM06-WP: Marine geological cruise to West Spitsbergen Margin and Fram Strait. Department of Geology, University of Tromsø, Norway.
- Husum, K., 2007. CRUISE REPORT JM07-WP: Marine geological cruise to East Greenland Margin. Department of Geology, University of Tromsø, Norway.
- Husum, K. and Hald, M., 2004. A continuous marine record 8000-1600 cal. yr BP from the Malangenfjord, north Norway: foraminiferal and isotopic evidence. *The Holocene* 14(6), 877-887.
- IPCC, 2007. *Climate Change 2007: The Physical Science Basis. Contribution of Working Group I to the Fourth Assessment Report of the Intergovernmental Panel on Climate Change* [Solomon, S., D. Qin, M. Manning, Z. Chen, M. Marquis, K.B. Averyt, M. Tignor and H.L. Miller (eds.)]. Cambridge University Press, Cambridge, United Kingdom and New York, NY, USA. IPCC, Genève, Suisse.
- Jennings, A.E. et N.J. Weiner. 1996. Environmental change in eastern Greenland during the last 1300 years: evidence from foraminifera and lithofacies in Nansen Fjord, 68°N. *The Holocene*, 6(2), 179-191.
- Jiang, H., Seidenkrantz, M.S., Knudsen, K.L. and Eriksson, J., 2002. Late-Holocene summer sea-surface temperatures based on a diatom record from the north Icelandic shelf. *The Holocene* 12(2), 137-147.
- Karlén, W. and Kuylensstierna, J., 1996. On solar forcing of Holocene climate: evidence from Scandinavia. *The Holocene* 6(3), 359-365.

- Komuro, Y. and Hasumi, H., 2007. Effects of variability of sea ice transport through the Fram Strait on the intensity of the Atlantic deep circulation. *Climate Dynamics* 29(5), 455-467.
- Krauss, W., Fahrbach, E., Aitsam, A., Elken, J. and Koshe, P., 1987. The North Atlantic current and its associated eddy field southeast of Flemish Cap. Deep-sea research. Part A. *Oceanographic research papers* 34(7), 1163-1185.
- Kucera, M., Weinelt, M., Kiefer, T., Pflaumann, U., Hayes, A., Weinelt, M., Chen, M.T., Mix, A.C., Barrows, T.T. and Cortijo, E., 2005. Reconstruction of sea-surface temperatures from assemblages of planktonic foraminifera: multi-technique approach based on geographically constrained calibration data sets and its application to glacial Atlantic and Pacific Oceans. *Quaternary Science Reviews* 24(7-9), 951-998.
- MacDonald, G.M., Velichko, A.A., Kremenetski, C.V., Borisova, O.K., Goleva, A.A., Andreev, A.A., Cwynar, L.C., Riding, R.T., Forman, S.L. and Edwards, T.W.D., 2000. Holocene Treeline History and Climate Change Across Northern Eurasia. *Quaternary Research* 53(3), 302-311.
- Malmgren, B.A. and Nordlund, U., 1997. Application of artificial neural networks to paleoceanographic data. *Palaeogeography, Palaeoclimatology, Palaeoecology* 136(1), 359-373.
- Matthews, J., 1969. The assessment of a method for the determination of absolute pollen frequencies. *New Phytologist* 68(1), 161-166.
- McDermott, F., Mathey, D.P., and Hawkesworth, C., 2001. Centennial-scale Holocene climate variability revealed by a high-resolution speleothem $\delta^{18}\text{O}$ record from SW Ireland. *Science* 294, 1328-1331.
- Mikalsen, G., H.P. Sejrup, et I. Aarseth. 2001. Late-Holocene changes in ocean circulation and climate: foraminiferal and isotopic evidence from Sulafjord, western Norway. *The Holocene*, 11(4), 437-446.
- NODC (National Oceanographic Data Center), 2001. World Ocean Database 2001, Scientific Data Sets, Observed and Standard Level Oceanographic Data [CD-Rom], National Oceanic and Atmospheric Administration.
- NSIDC (National Snow and Ice Data Center), 2003. Brightness temperature and ice concentrations grids for the polar regions. User's guide. NSIDC Distributed Active Archive Center, University of Colorado, Boulder.

- Nesje, A., Matthews, J.A., Dahl, S.O., Bërrisford, M.S. and Andersson, C., 2001. Holocene glacier fluctuations of Flatebreen and winter-precipitation changes in the Jostedalsbreen region, western Norway, based on glaciolacustrine sediment records. *The Holocene* 11(3), 267-280.
- O'Brien, S.R., Mayewski, P.A., Meeker, L.D., Meese, D.A., Twickler, M.S. and Whitlow, S.I., 1995. Complexity of Holocene Climate as Reconstructed from a Greenland Ice Core. *Science* 270(5244), 1962-1964.
- Peyron, O. and De Vernal, A., 2001. Application of artificial neural networks (ANN) to high latitude dinocyst assemblages for the reconstruction of past sea-surface conditions in Arctic and sub-Arctic seas. *Journal of Quaternary Science* 16(7), 699-709.
- Rochon, A., de Vernal, A., Turon, J.-L., Matthiessen, J. and Head, M.J., 1999. Distribution of Recent Dinoflagellate Cysts in Surface Sediments from the North Atlantic Ocean and Adjacent Seas in Relation to Sea-surface Parameters. American Association of Stratigraphic Palynologists Foundation.
- Rousse, S., Kissel, C., Laj, C., Eiríksson, J. and Knudsen, K.L., 2006. Holocene centennial to millennial-scale climatic variability: Evidence from high-resolution magnetic analyses of the last 10 cal kyr off North Iceland (core MD99-2275). *Earth and Planetary Science Letters* 242(3-4), 390-405.
- Rudels, B., Björk, G., Nilsson, J., Winsor, P., Lake, I. and Nohr, C., 2005. The interaction between waters from the Arctic Ocean and the Nordic Seas north of Fram Strait and along the East Greenland Current: results from the Arctic Ocean-02 Oden expedition. *Journal of Marine Systems* 55(1-2), 1-30.
- Schauer, U., Loeng, H., Rudels, B., Ozhigin, V.K. and Dieck, W., 2002. Atlantic Water flow through the Barents and Kara Seas. *Deep-Sea Research Part I* 49(12), 2281-2298.
- Seppä, H. and Birks, H.J.B., 2002. Holocene Climate Reconstructions from the Fennoscandian Tree-Line Area Based on Pollen Data from Toskaljavri. *Quaternary Research* 57(2), 191-199.
- Ślubowska-Woldengen, M.A., Rasmussen, T.L., Koç, N., Klitgaard-Kristensen, D., Nilsen, F. and Solheim, A., 2007. Advection of Atlantic Water to the western and northern Svalbard shelves through the last 17.5 ka cal yr BP. *Quaternary Science Reviews* 26, 463-478.

- Solignac, S., de Vernal, A. and Hillaire-Marcel, C., 2004. Holocene sea-surface conditions in the North Atlantic—contrasted trends and regimes in the western and eastern sectors (Labrador Sea vs. Iceland Basin). *Quaternary Science Reviews* 23(3-4), 319-334.
- Stuiver, M., Reimer, P.J., and Reimer, R., 2000. CALIB radiocarbon calibration HTML version 5.0.2 and marine correction data base, <http://calib.qub.ac.uk/calib/>.
- Taylor, F.J.R. and Pollinger, U., 1987. Ecology of dinoflagellates. In: Taylor, F.J.R. (Eds.), *The biology of dinoflagellates*. Blackwell Scientific, Oxford, pp. 398-529.
- Telford, R.J., 2006. Limitations of dinoflagellate cyst transfer functions, *Quaternary Science Reviews* 25, 1375-1382.
- Walczowski, W., Piechura, J., Osinski, R. and Wieczorek, P., 2005. The West Spitsbergen Current volume and heat transport from synoptic observations in summer. *Deep-Sea Research Part I* 52(8), 1374-1391.

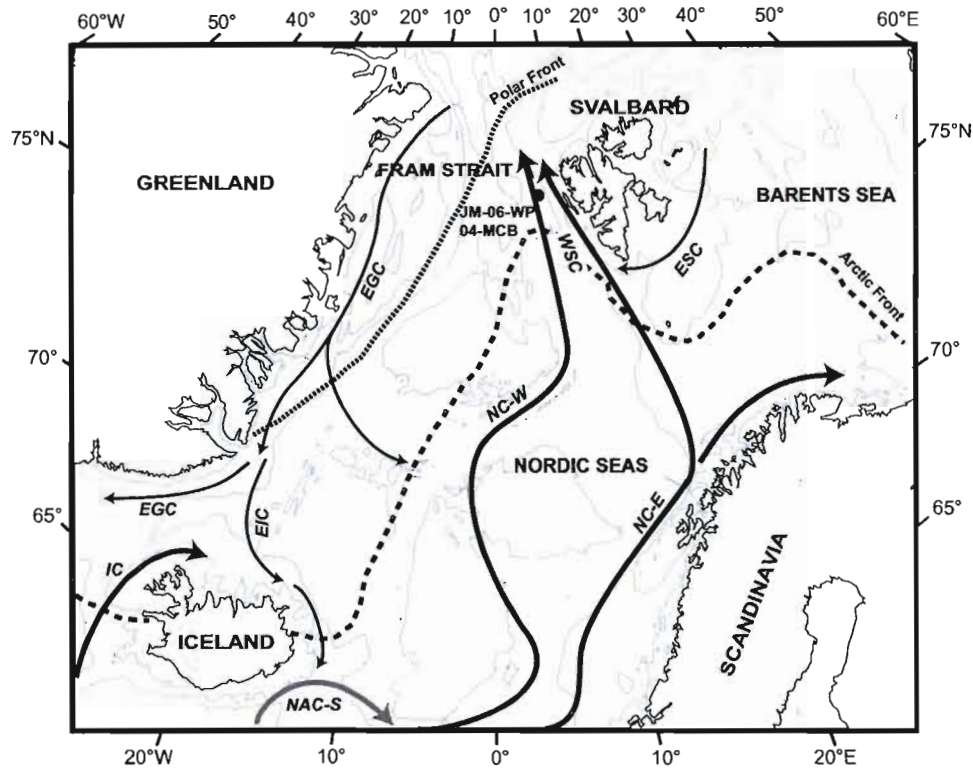


Figure 1. Location of core JM-06-WP-04-MCB (JM04; 78.92°N, 6.77°E, water depth: 1497 m, core length: 54 cm) and trajectories of main ocean surface currents (cf. Hansen and Østerhus, 2000). Thick arrows depict warm currents and thin arrows, cold currents. Respectively, the dashed line and dotted line represent the Arctic and Polar Front, which are associated to the maximum sea-ice extension in winter and summer as defined from the 1953-2001 data set provided by the National Snow and Ice Data Center (NSIDC, 2001). Isobaths correspond to 200, 1000 and 3000 m. EGC: East Greenland Current, EIC: East Icelandic Current, ESC: East Spitsbergen Current, NC-E: eastern branch of the Norwegian Current, NC-W: western branch of the Norwegian Current, WSC: West Spitsbergen Current, NAC-S: southern branch of the North Atlantic Current, IC: Irminger Current.

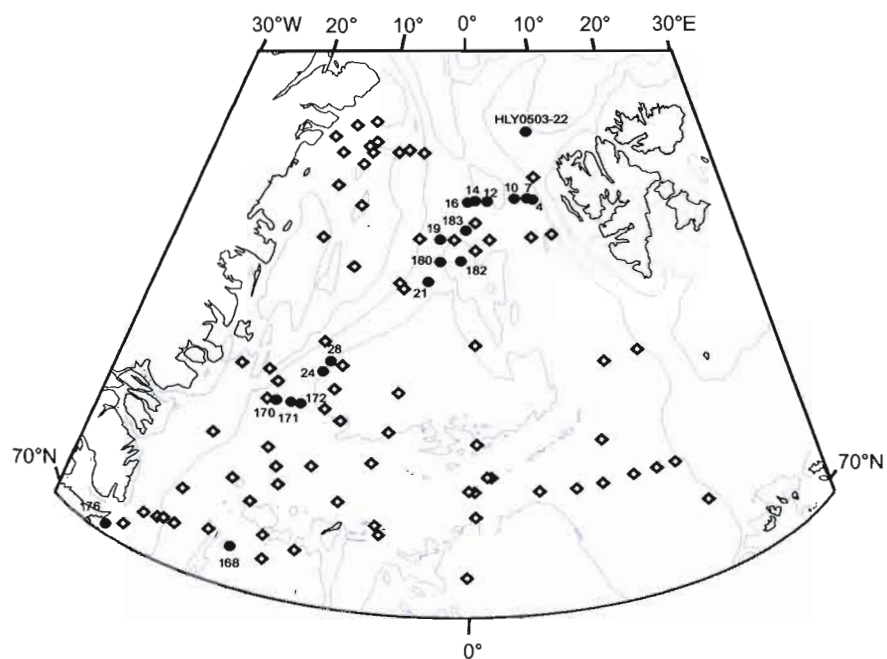


Figure 2. Location map of the surface sediment samples used for canonical correspondence analysis (cf. Figure 6). Diamonds: data from de Vernal et al. (2005); circles: data from new reference sites (cf. Table 1). Isobaths correspond to 200, 1000 and 3000 m.

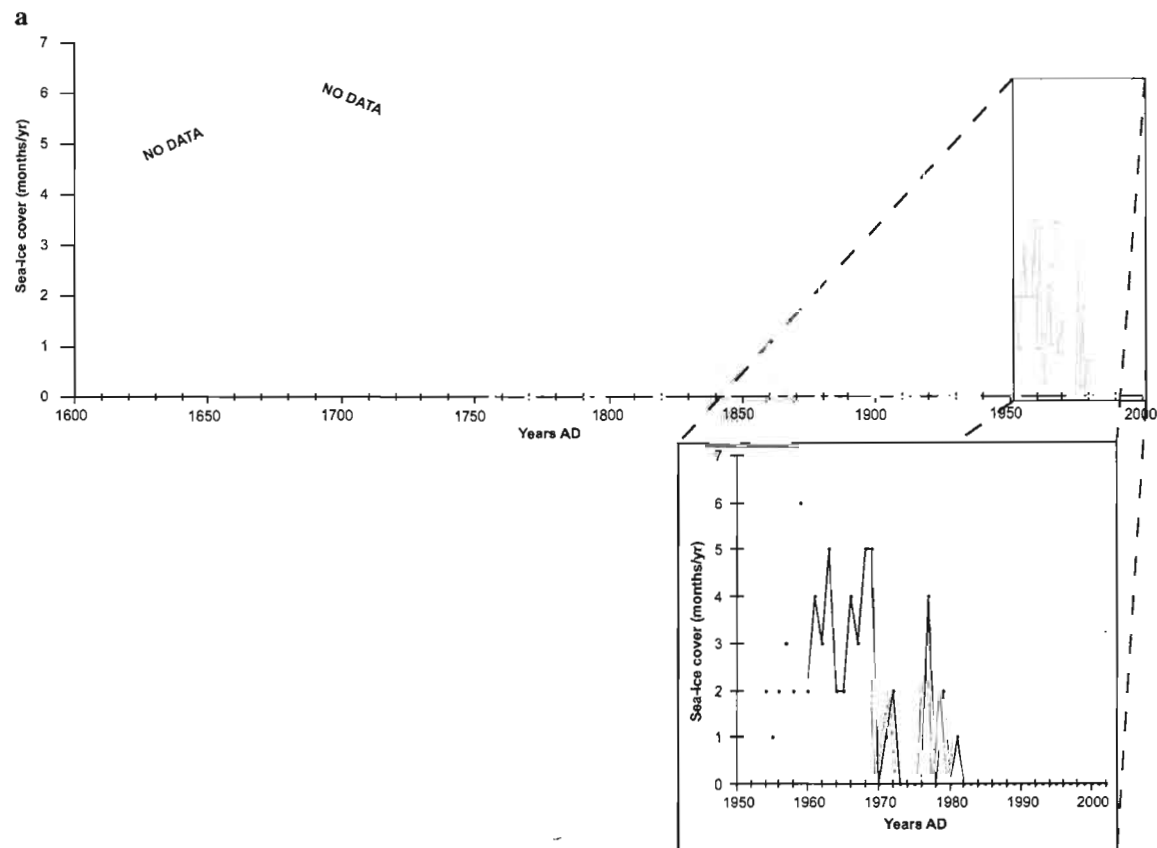


Figure 3. a) Historical records of sea-ice cover with concentration greater than 30% as a function of years for the period AD 1596-2002 at the site of core JM04. The close-up represents the sea-ice cover with concentration greater than 50% as a function of years for the period AD 1953-2001 (black curve). These data are provided by the NSIDC (2001). The grey curve illustrates historical records for the period AD 1953-2002. Data are compiled from ACSYS (2003). Note the important variability of sea-ice cover and its absence since 1982.

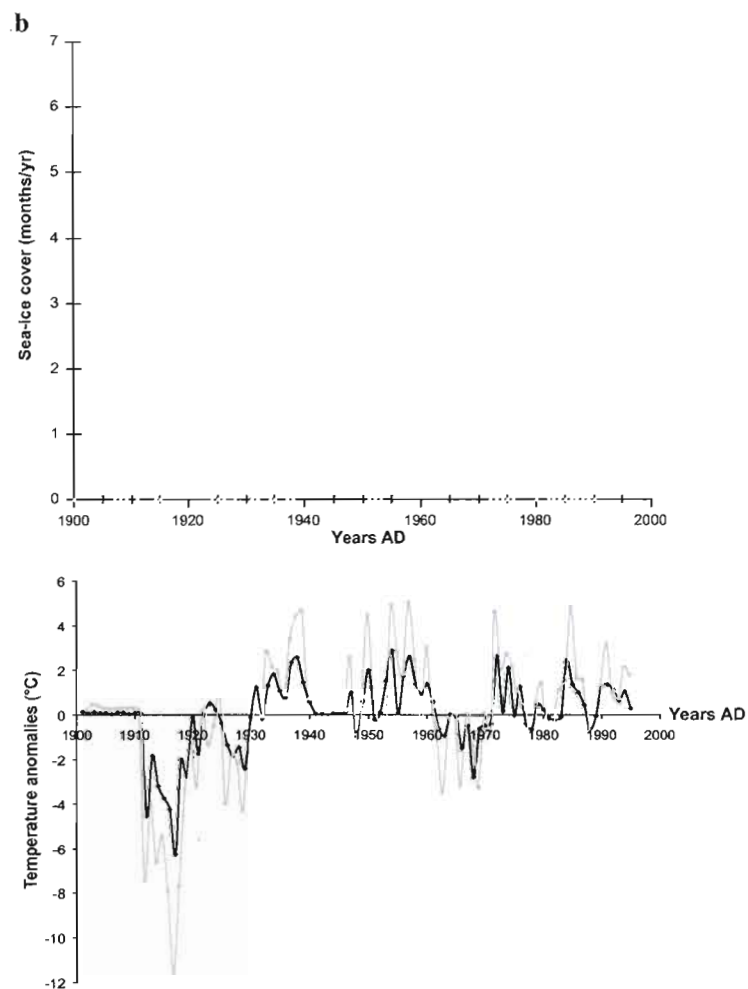


Figure 3. **b)** Historical sea-ice records for the period AD 1900-2002 and mean annual (black curve) and mean winter (December to March; grey curve) air temperature anomalies (°C) between 1901 and 1995 in this area (75-80°N; 5-11°E). Annual and winter temperatures are, respectively, $-8.35 \pm 1.57^{\circ}\text{C}$ and $-16.03 \pm 2.92^{\circ}\text{C}$.

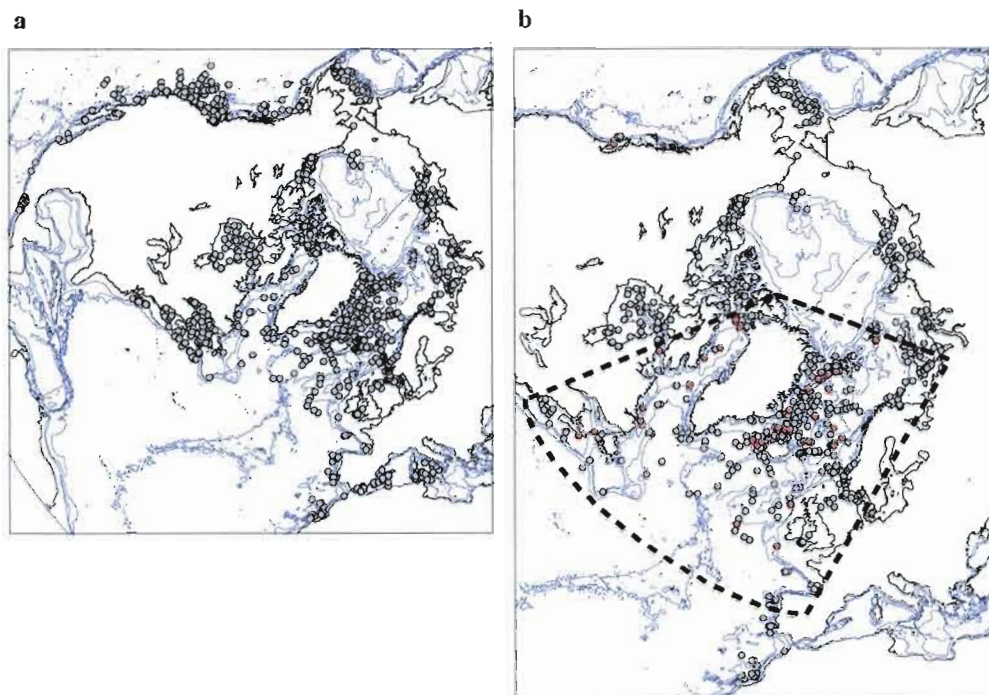


Figure 4. Location map of surface sediment samples used to reconstruct past sea-surface conditions from dinocyst assemblages in core JM04. **a)** Reference database used for MAT (n=1208 sites). **b)** Calibration databases for ANN: one includes all sites from the North Atlantic and Arctic (n=735 sites). The other one includes sites from the area delimited by the dashed line (n=437 sites), as defined from the best analogues selected using MAT (red points).

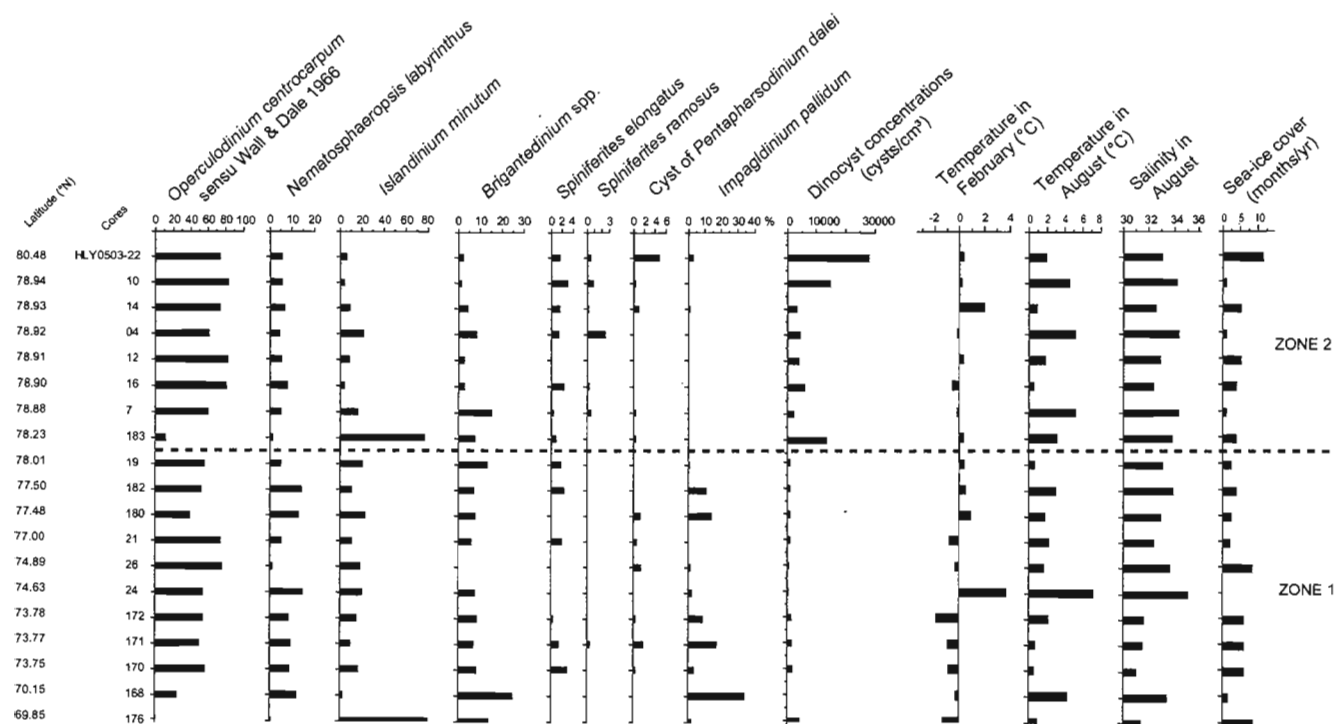


Figure 5. Percentage diagram of dinocyst taxa in surface sediment samples ranked by latitude (cf. Figure 2 for location). Different scales were used for dominant and accompanying taxa. Percentages of taxa with occasional occurrence lower than 1% are not reported. Dinocyst concentrations and modern sea-surface conditions (cf. National Ocean Data Center (NODC) and NSIDC, 2001) are indicated on the right of the diagram.

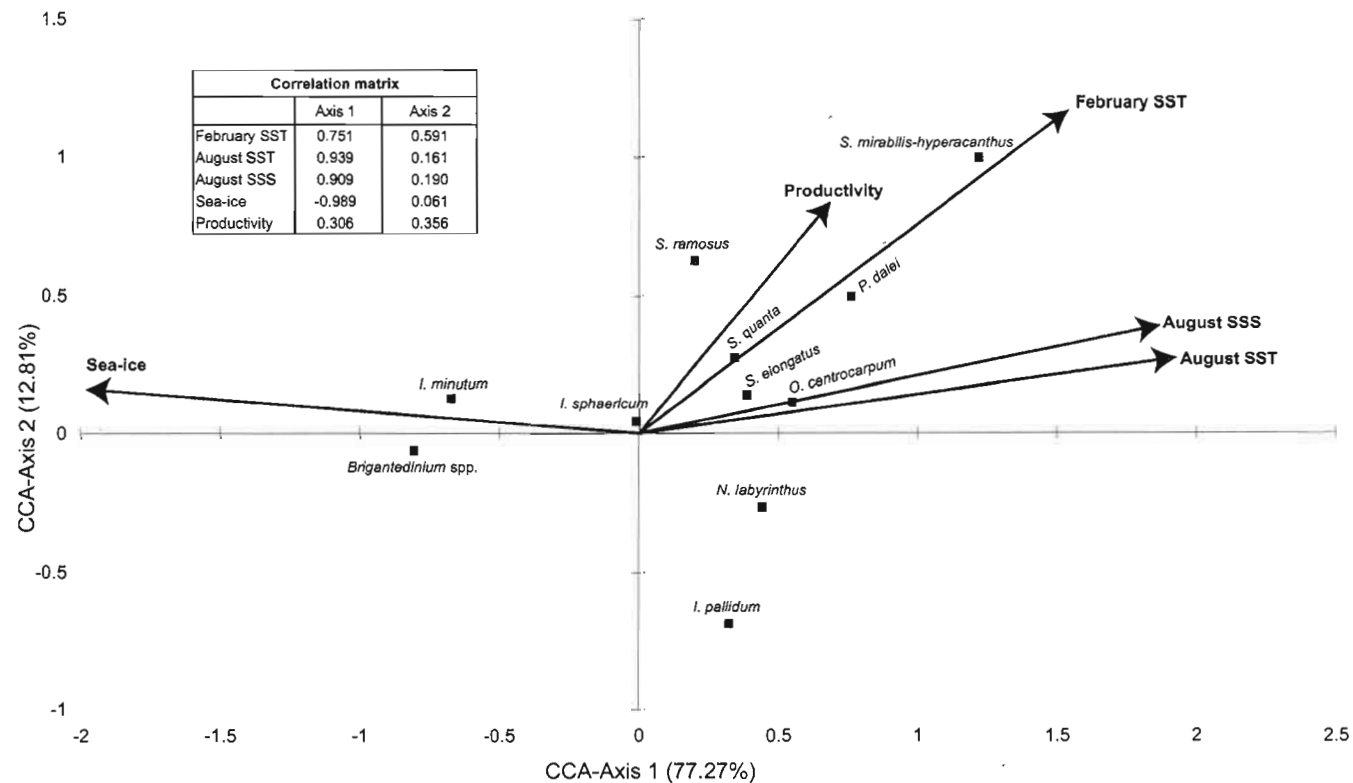


Figure 6. Results of CCA analysis. Ordination diagram of dinocyst taxa and environmental variables according to axis 1 and 2, and Pearson cross-correlation matrix between these two axes and hydrographical parameters. This analysis was performed with the XLSTAT software (Addinsoft, 2008), using the 94 sites (cf. Figure 2).

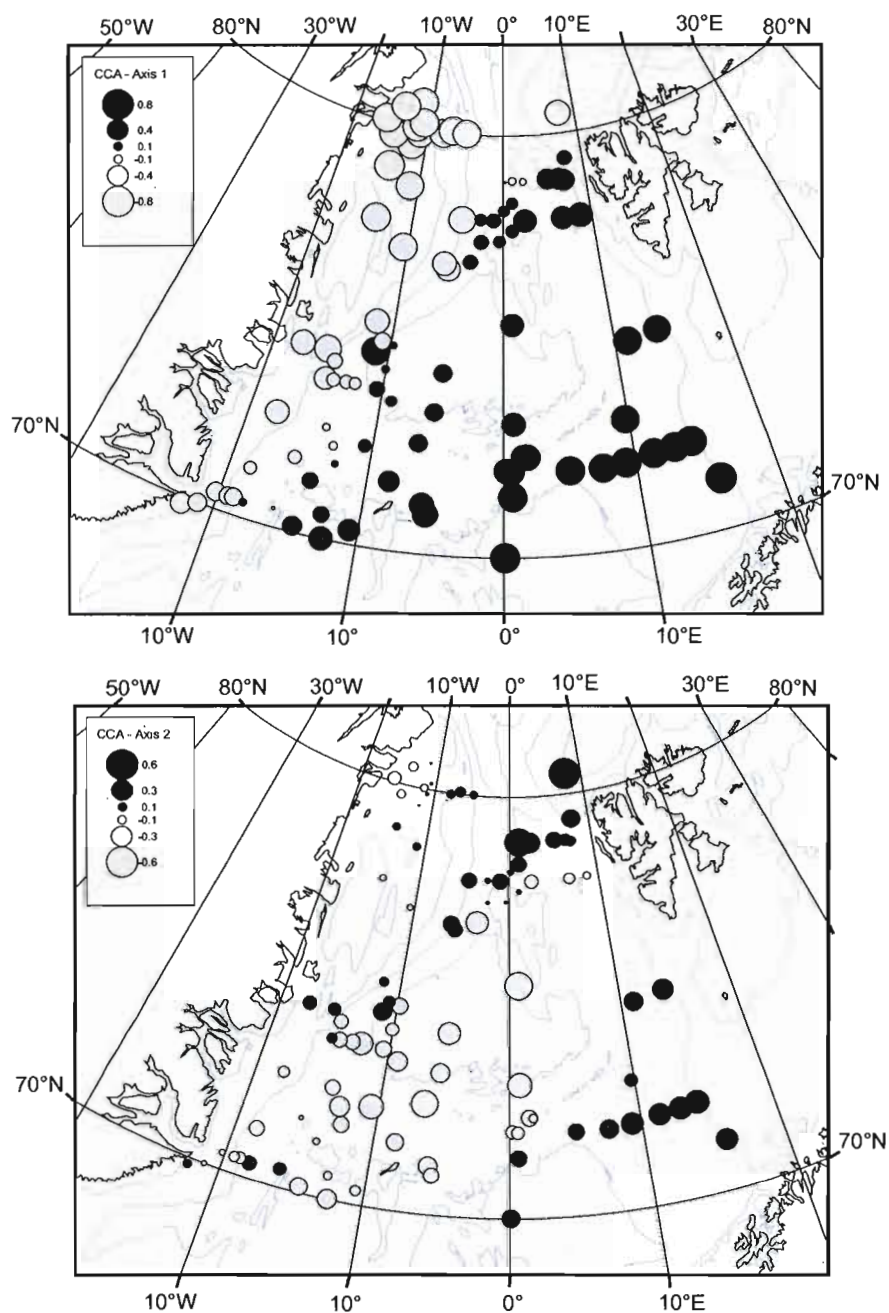


Figure 7. Geographical distribution of the scores for CCA axes 1 and 2, which represent, respectively, 77.27% and 12.81% of the total variance. Isobaths correspond to 200, 1000 and 3000 m.

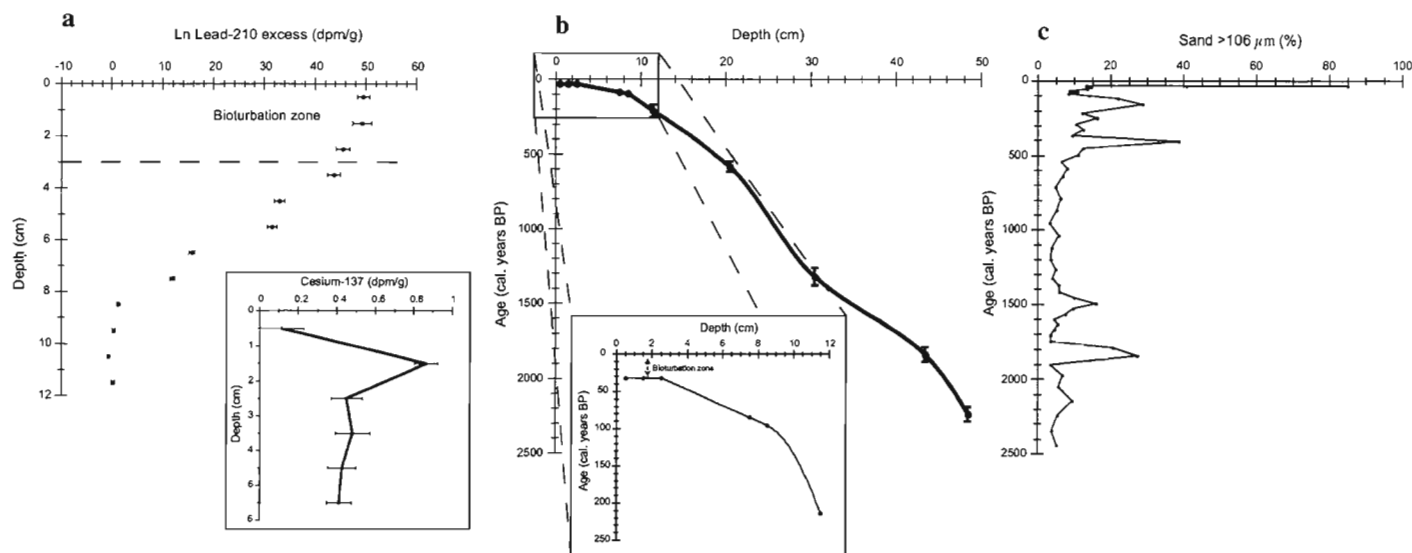


Figure 8. a) Ln Lead-210 excess and Cesium-137 activities as a function of depth in core JM04. b) Age model of core JM04. The five dots with error bars represent calibrated Carbon-14 ages (see Table 2). The black line shows the interpolated ages vs. depth relationship, which was used to establish the chronology in the core (Figures 9, 10 and 12). From 11.5 cm to the base of the core, we calculate mean sedimentation rate of 18 cm/kyrs. The close-up of depth vs. age for the upper 12 cm of the core shows the age model based on Lead-210. c) Percentage of the coarse sand fraction (>106 μm) as a function of age.

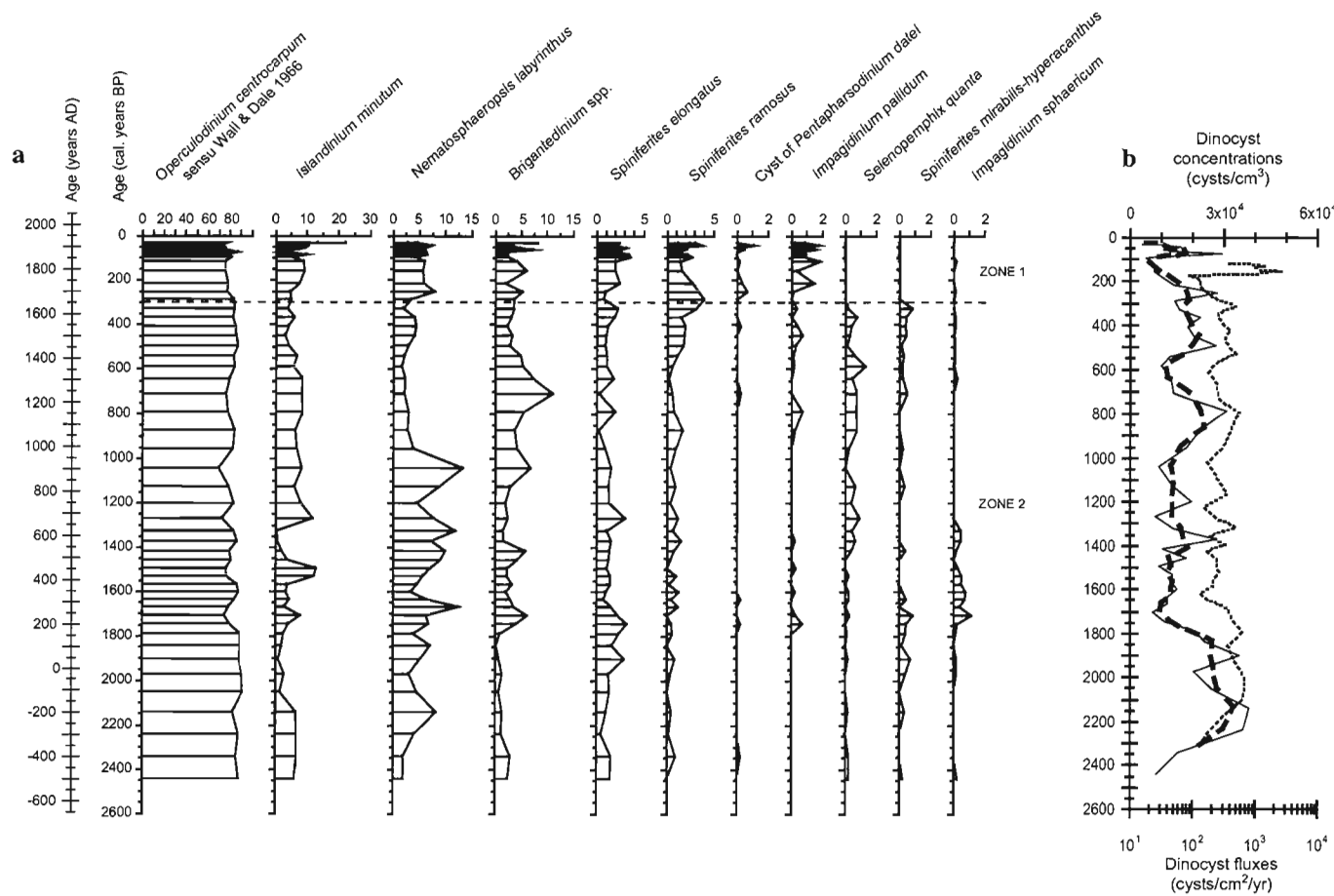


Figure 9. a) Diagram of dinocyst taxa percentages as a function of age in core JM04. Different scales were used for dominant and accompanying taxa. Two assemblage zones separated by the horizontal dashed line were defined on the basis of the principal component analysis calculations (cf. Figure 10). b) Dinocyst concentrations (solid line) and fluxes (dotted line). The thick dashed line correspond to smoothed concentration values (three-point running average).

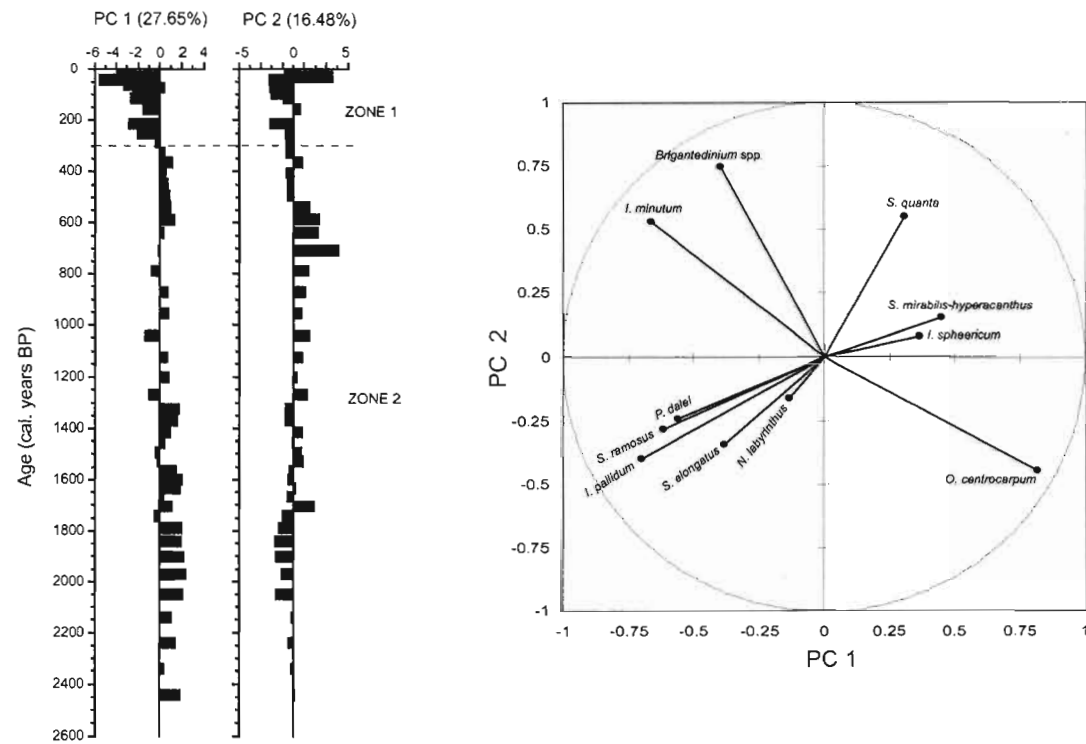


Figure 10. Principal components 1 and 2 (PC 1 and PC 2) as a function of age (left) and ordination diagram of dinocyst taxa based on PC 1 and PC 2 (right) for core JM04.

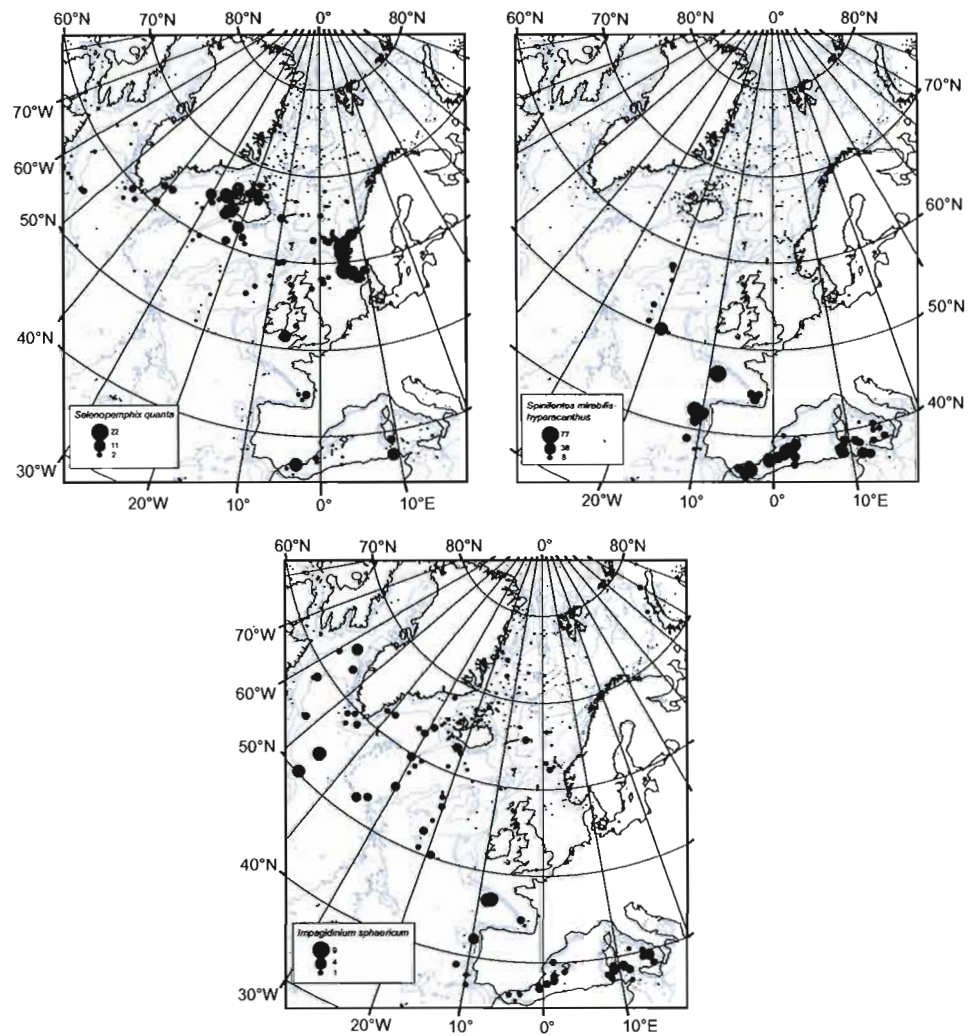


Figure 11. Distribution maps of *Selenopemphix quanta*, *Spiniferites mirabilis-hyperacanthus* and *Impagidinium sphaericum* in surface sediment samples of the northern North Atlantic. Occurrences are expressed in percentages. Isobaths correspond to 200, 1000 and 3000 m.

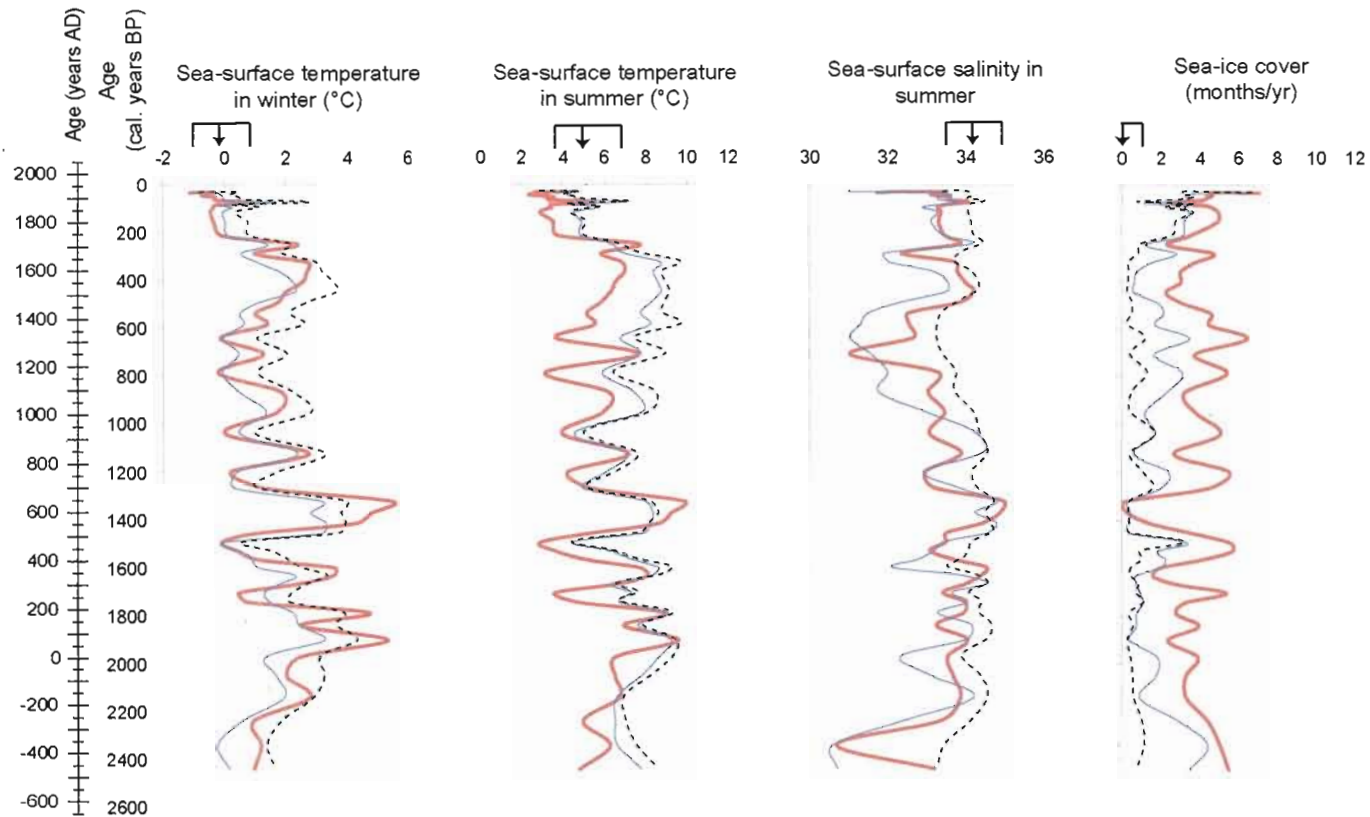


Figure 12. Reconstruction of sea-surface conditions (temperatures, salinity, sea-ice cover) from dinocyst assemblages for the last 2500 years as a function of age, based on MAT and ANN techniques. The overall reference database (n=1208 sites) was used for MAT (red line), the North Atlantic and Arctic database with n=735 sites was used for ANN (blue line) as well as the database delimited by the analogues with n=437 sites (dashed line) (cf. Figure 4 for calibration databases). The modern values with their standard deviations are represented by $\boxed{\downarrow}$.

Table 1. Location of surface sediment samples and core JM-06-WP-04-MCB

Cruises	Cores	Abbreviation indicated on fig. 2 and 5	Sampling type	Latitude (°N)	Longitude	Water depth (m)
HOTRAX 2005	HL0503-22MC-8	HL0503-22	Multicore	80.48	7.77	798
Warm Past 2006	JM06-WP-10-BCB	10	Boxcore	78.94	5.4	2483
Warm Past 2006	JM06-WP-14-BCE	14	Boxcore	78.93	1.11	2502
Warm Past 2006	JM06-WP-04-MCB	4	Multicore	78.92	6.77	1497
Warm Past 2006	JM06-WP-12-BCB	12	Boxcore	78.91	2.42	2426
Warm Past 2006	JM06-WP-16-MCB	16	Multicore	78.9	0.28	2546
Warm Past 2006	JM06-WP-7-BCC	7	Boxcore	78.88	7.34	1181
Warm Past 2007	JM07-WP-183-MCB	183	Multicore	78.23	0.1	340
Warm Past 2006	JM06-WP-19-MCB	19	Multicore	78.01	-2.5	2859
Warm Past 2007	JM07-WP-182-MCB	182	Multicore	77.5	-0.4	3100
Warm Past 2007	JM07-WP-180-MCB	180	Multicore	77.48	-2.4	3029
Warm Past 2006	JM06-WP-21-MCE	21	Multicore	77	-3.39	1779
Warm Past 2006	JM06-WP-26-MCC	26	Multicore	74.89	-10.77	3064
Warm Past 2006	JM06-WP-24-MCA	24	Multicore	74.63	-11.19	2974
Warm Past 2007	JM07-WP-172-MCB	172	Multicore	73.78	-12.35	2742
Warm Past 2007	JM07-WP-171-MCB	171	Multicore	73.77	-13.1	2570
Warm Past 2007	JM07-WP-170-MCB	170	Multicore	73.75	-14.2	2285
Warm Past 2007	JM07-WP-168-MCB	168	Multicore	70.15	-14.52	332
Warm Past 2007	JM07-WP-176-MCB	176	Multicore	69.85	-22.13	482

Table 2. Radiocarbon ages determined for the core JM-06-WP-04-MCB. The software Calib 5.0.2 (Stuiver et al., 2000) was used for calibration with a reservoir correction of 400 years and normalization for a $\delta^{13}\text{C}$ of -25‰ PDB (Stuiver et al., 2000)

Depth (cm)	Material dated	Uncorrected AMS- ^{14}C ages (years BP)	Calibrated age interval (1 σ) (years BP)	Calibrated age interval (1 σ) (years AD/BC)	Laboratory	Laboratory number
11-12	<i>Neogloboquadrina pachyderma</i> and <i>Globigerina bulloides</i>	560 \pm 35	173-254	AD 1696 - AD 1777	Lawrence Livermore National Laboratory	140961
20-21	<i>Neogloboquadrina pachyderma</i> and <i>Globigerina bulloides</i>	1005 \pm 35	551-622	AD 1328 - AD 1399	Lawrence Livermore National Laboratory	140962
30-31	<i>Neogloboquadrina pachyderma</i>	1790 \pm 25	1294-1353	AD 597 - AD 656	Leibniz Laboratory, Kiel (Germany)	KJA-33880
43-44	<i>Neogloboquadrina pachyderma</i> and <i>Globigerina bulloides</i>	2235 \pm 35	1792-1889	AD 61 - AD 158	Lawrence Livermore National Laboratory	140963
48-49	<i>Neogloboquadrina pachyderma</i>	2555 \pm 25	2189-2289	340 BC - 240 BC	Leibniz Laboratory, Kiel (Germany)	KJA-34274

Table 3. Results of validation tests of sea-surface temperatures, salinity and sea-ice cover reconstructions based on MAT and ANN (databases of Atlantic+Arctic sites and according to the analogues). R^2 corresponds to the correlation coefficient between observed and estimated values. RMSE (Root Mean Square error) is the standard deviation of the difference between observed and estimated values. RMSEP (Root Mean Square Error of Prediction) is calculated by dividing the database in calibration and verification data sets

ENVIRONMENTAL PARAMETERS	TRANSFER FUNCTIONS											
	MAT (10 analogues)				ANN (Atlantic + Arctic) 5 hidden layers. 5000 iterations				ANN (according to the analogues) 5 hidden layers. 2000 iterations			
	σ	R^2	RMSE	RMSEP	σ	R^2	RMSE	RMSEP	σ	R^2	RMSE	RMSEP
February temperature	1.10	0.97	1.21	1.03	1.15	0.93	1.12	1.46	1.11	0.91	1.10	1.50
Winter temperature	1.08	0.97	1.19	0.96	1.13	0.94	1.10	1.45	1.09	0.92	1.09	1.52
August temperature	1.66	0.95	1.82	1.59	1.98	0.87	1.96	1.98	1.72	0.90	1.66	2.10
Summer temperature	1.55	0.95	1.71	1.52	1.82	0.89	1.79	1.88	1.62	0.91	1.58	2.04
August salinity (>30)	0.67	0.89	0.67	0.73	0.72	0.83	0.70	0.93	0.67	0.83	0.65	0.94
Summer salinity (>30)	0.63	0.90	0.62	0.73	0.67	0.85	0.65	0.88	0.62	0.85	0.59	0.91
Sea-ice cover	1.19	0.89	1.24	1.18	1.52	0.88	1.46	1.73	1.11	0.90	1.05	1.90

Table 4. Distance of the ten closest analogues for the core JM-06-WP-04-MCB as a function of depth, obtained with MAT. The threshold value for poor analogues is 1.31

Depth (cm)	Distance of the ten closest analogues									
	1	2	3	4	5	6	7	8	9	10
0	0.23	0.37	0.39	0.48	0.50	0.53	0.55	0.56	0.56	0.57
1	0.18	0.26	0.40	0.41	0.45	0.50	0.51	0.51	0.52	0.53
2	0.31	0.38	0.40	0.48	0.49	0.50	0.52	0.55	0.55	0.57
3	0.29	0.32	0.32	0.34	0.35	0.35	0.36	0.37	0.41	0.41
4	0.19	0.29	0.36	0.37	0.39	0.43	0.45	0.45	0.45	0.45
5	0.28	0.33	0.34	0.35	0.36	0.37	0.39	0.39	0.41	0.41
6	0.24	0.35	0.37	0.37	0.39	0.39	0.41	0.42	0.43	0.46
7	0.32	0.36	0.38	0.46	0.48	0.50	0.50	0.51	0.53	0.54
8	0.31	0.36	0.39	0.43	0.48	0.49	0.53	0.56	0.57	0.57
9	0.31	0.33	0.35	0.35	0.36	0.37	0.38	0.38	0.38	0.38
10	0.23	0.30	0.43	0.43	0.44	0.45	0.47	0.49	0.53	0.53
11	0.28	0.31	0.38	0.40	0.40	0.40	0.43	0.44	0.44	0.45
12	0.38	0.39	0.40	0.40	0.43	0.43	0.43	0.43	0.44	0.46
13	0.31	0.42	0.48	0.49	0.50	0.57	0.58	0.61	0.61	0.61
14	0.39	0.39	0.49	0.56	0.56	0.58	0.59	0.59	0.60	0.61
15	0.35	0.44	0.50	0.51	0.53	0.55	0.55	0.57	0.58	0.58
16	0.37	0.38	0.39	0.40	0.42	0.44	0.45	0.46	0.48	0.49
17	0.34	0.41	0.42	0.43	0.45	0.45	0.51	0.51	0.52	0.52
18	0.33	0.37	0.39	0.42	0.44	0.47	0.52	0.54	0.54	0.56
19	0.28	0.41	0.46	0.48	0.49	0.51	0.52	0.53	0.54	0.54
20	0.26	0.41	0.42	0.43	0.46	0.49	0.49	0.49	0.51	0.51
21	0.14	0.39	0.40	0.42	0.43	0.45	0.47	0.48	0.51	0.52
22	0.29	0.33	0.39	0.41	0.43	0.44	0.46	0.47	0.47	0.48
23	0.33	0.41	0.45	0.45	0.50	0.51	0.51	0.53	0.55	0.55
24	0.37	0.40	0.43	0.43	0.47	0.47	0.50	0.51	0.54	0.55
25	0.24	0.45	0.46	0.46	0.47	0.48	0.49	0.54	0.54	0.55
26	0.15	0.40	0.41	0.42	0.42	0.45	0.47	0.47	0.49	0.53
27	0.35	0.43	0.48	0.50	0.50	0.51	0.52	0.53	0.56	0.57
28	0.20	0.40	0.43	0.45	0.45	0.46	0.47	0.49	0.51	0.52
29	0.32	0.46	0.47	0.52	0.52	0.53	0.54	0.56	0.56	0.57
30	0.19	0.25	0.31	0.34	0.39	0.39	0.40	0.42	0.44	0.44
31	0.21	0.24	0.34	0.38	0.40	0.43	0.43	0.45	0.45	0.46
32	0.30	0.33	0.36	0.37	0.41	0.41	0.44	0.45	0.47	0.47
33	0.20	0.41	0.42	0.42	0.48	0.49	0.49	0.49	0.50	0.50
34	0.22	0.31	0.34	0.36	0.37	0.38	0.38	0.39	0.39	0.40
35	0.34	0.40	0.49	0.51	0.54	0.57	0.58	0.60	0.60	0.61
36	0.20	0.37	0.38	0.44	0.45	0.46	0.50	0.51	0.53	0.53
37	0.39	0.40	0.41	0.46	0.49	0.53	0.53	0.53	0.55	0.56
38	0.35	0.37	0.39	0.39	0.40	0.42	0.46	0.47	0.50	0.51
39	0.30	0.34	0.40	0.46	0.52	0.53	0.53	0.53	0.54	0.54
40	0.36	0.44	0.49	0.50	0.54	0.56	0.56	0.56	0.56	0.57
41	0.31	0.32	0.37	0.38	0.40	0.40	0.41	0.41	0.41	0.43
42	0.35	0.38	0.42	0.42	0.43	0.43	0.44	0.48	0.49	0.50
43	0.38	0.40	0.40	0.43	0.44	0.45	0.48	0.49	0.51	0.52
44	0.32	0.34	0.37	0.38	0.39	0.42	0.44	0.46	0.46	0.47
45	0.26	0.38	0.39	0.44	0.46	0.47	0.47	0.48	0.49	0.51
46	0.26	0.31	0.32	0.33	0.38	0.39	0.44	0.44	0.47	0.47
47	0.29	0.42	0.44	0.44	0.49	0.51	0.51	0.53	0.55	0.55
48	0.22	0.41	0.41	0.45	0.48	0.48	0.50	0.52	0.54	0.54
49	0.23	0.25	0.33	0.39	0.42	0.42	0.43	0.43	0.44	0.45
50	0.16	0.36	0.42	0.43	0.45	0.49	0.49	0.51	0.51	0.54

CONCLUSION GÉNÉRALE

Fiabilité des dinokystes comme proxy

Dans le cadre de cette thèse, nous avons pu confirmer le potentiel des dinokystes comme proxy pour les reconstitutions paléoenvironnementales dans les hautes latitudes. Ils se révèlent particulièrement utiles dans les régions polaires et subpolaires pour retracer l'évolution du couvert de glace de mer. En effet, l'abondance de certains taxons hétérotrophes comme *Islandinium minutum* semble être reliée à la présence d'un couvert de glace saisonnier. En ce qui concerne la région du détroit de Fram, les dinokystes sont bien préservés dans les sédiments et constituent des assemblages relativement diversifiés. Par conséquent, ils représentent un excellent proxy pour les reconstitutions des conditions de surface océanique et de la glace de mer. Ainsi, les résultats d'analyse multivariée (*i.e.*, analyse canonique des correspondances) obtenus avec les assemblages de dinokystes des sédiments de surface (détroit de Fram et mers nordiques) illustrent une distribution géographique étroitement liée à l'étendue du couvert de glace de mer et à la circulation océanique de surface, avec le courant Est groenlandais exportant des eaux dessalées et froides de l'Arctique, à l'Ouest, et le courant Ouest Spitsberg apportant des masses d'eau plus chaudes et salées de l'Atlantique Nord, à l'Est.

Fonctions de transfert : validation des approches

Deux techniques ont été testées et utilisées pour reconstituer quantitativement les conditions de surface à partir des assemblages de dinokystes. La technique des meilleurs analogues (MAT) et celle des réseaux neuronaux (ANN). Les résultats des tests de validation indiquent que la méthode des analogues modernes est la plus fiable avec des erreurs de prédictions inférieures à celles obtenues avec les réseaux neuronaux. Lorsque utilisées à partir des assemblages de la carotte JM04, les deux techniques livrent des températures similaires. Par contre, la salinité et la glace de

mer présentent des différences. Pour la salinité, un biais positif ou négatif est observé avec ANN selon la base de données de calibration. Pour ce qui concerne la glace de mer, ANN livre des valeurs systématiquement plus faibles que MAT. Les données historiques de glace de mer disponibles pour la période 1553-2002 (ACSYS, 2003) confirment la validité des reconstitutions de MAT. Elles révèlent en effet un couvert de glace de mer moyen entre 4 et 3 mois/an, ce qui correspond aux reconstitutions de MAT alors que ANN indique une moyenne de 1 mois/an.

Variabilité des derniers 2500 ans dans le détroit de Fram

La carotte JM04, analysée à 1 cm d'intervalle, représente une période de 2500 ans sur une longueur de 50 cm avec un taux de sédimentation variable allant de 18 cm/10³ ans à 94 cm/10³ ans dans la partie supérieure (0-8 cm). La résolution temporelle est de l'ordre d'une centaine d'années. Ainsi, la carotte JM04 constitue un enregistrement unique, avec une telle résolution, pour la température et la salinité de surface ainsi que pour la glace de mer. Dans l'ensemble, les températures sont plus chaudes que l'actuel avec un couvert de glace de mer saisonnier de 4 mois/an, et deux événements climatiques majeurs marqués par (1) un optimum thermique pendant la Période Chaude Médiévale (PCM) vers 1320 ans cal. BP caractérisé par l'absence de glace de mer et (2) une sévère détérioration des conditions climatiques associée au Petit Âge Glaciaire (PAG) vers 300-250 ans cal. BP se traduisant par un refroidissement d'environ 3°C en Hiver et 5°C en Été. Au-delà de ces deux événements, plusieurs périodes froides sont observées vers 1700, 1500, 1200 et 800 ans cal. BP. Également, deux épisodes de faible salinité (< 31) sont enregistrés à 2340 et 700 ans cal. BP auxquels s'ajoute un épisode plus récent qui pourrait coïncider avec la grande anomalie de salinité observée dans l'Atlantique Nord dans les années 1970. L'épisode centré à 700 ans cal. BP serait associé à la mise en place de la première phase du PAG, ce qui concorde avec les autres études. Le refroidissement brutal vers 300 ans cal. BP correspondrait alors à sa dernière phase. Les oscillations

séculaires à millénaires de la température et salinité de surface ainsi que de la glace de mer montrent des instabilités qui sont reliées à la dynamique des flux de l'Arctique vers l'Atlantique Nord. Les épisodes de faible salinité auraient entraîné une diminution de la densité des eaux de surface et par conséquent, une réduction de la formation d'eau profonde dans les mers nordiques et donc de la circulation thermohaline. Cette étude démontre la sensibilité du climat dans la région du détroit de Fram et suggère des variations dans le débit relatif et/ou dans la latitude atteinte par le courant Nord Atlantique ainsi que des fluctuations dans la circulation thermohaline.

APPENDICE A

TABLEAUX DE COMPTAGES ET CONCENTRATIONS DES PALYNOMORPHES TERRESTRES ET MARINS DE LA CAROTTE JM-06-WP-04-MCB

Tableau A.1. Dénombrements et concentrations des dinokystes de la carotte JM-06-WP-04-MCB.....56

Tableau A.2. Dénombrements et concentrations des grains de pollen et des spores de la carotte JM-06-WP-04-MCB.....59

Tableau A.3. Dénombrements et concentrations des palynomorphes remaniés et des réseaux organiques de foraminifères benthiques de la carotte JM-06-WP-04-MCB.....62

Tableau A.1.
Dénombrements et concentrations des dinokystes de la carotte JM-06-WP-04-MCB

Profondeur (cm)	0	1	2	3	4	5	6	7	8	9	10	11	12	13	14	15	16
<i>Ataxiodinium choane</i>	0	0	0	0	0	0	0	0	0	0	0	0	0	0	0	0	0
<i>Impagidinium pallidum</i>	0	1	5	8	3	8	2	5	3	10	2	8	1	0	2	0	3
<i>Impagidinium paradoxum</i>	0	0	0	0	0	0	0	0	0	0	0	0	0	0	0	0	0
<i>Impagidinium sphaericum</i>	0	0	0	0	0	0	0	0	0	1	0	0	1	0	0	1	1
<i>Nematosphaeropsis labyrinthus</i>	13	11	23	33	31	28	25	34	14	32	31	31	49	17	12	25	33
<i>Operculodinium centrocarpum</i>	169	286	414	303	381	369	331	376	268	397	403	402	466	403	494	501	630
<i>Operculodinium centrocarpum</i> court processus	1	17	12	11	5	26	15	10	1	10	11	14	7	14	12	11	5
<i>Spiniferites elongatus</i>	4	10	11	9	16	14	10	18	12	11	11	13	6	4	14	12	9
<i>Spiniferites ramosus</i>	7	5	17	17	3	10	5	12	9	8	9	15	21	20	19	10	15
<i>Spiniferites mirabilis-hyperacanthus</i>	0	0	0	0	0	0	0	0	0	0	0	0	0	0	5	3	3
<i>Spiniferites</i> spp.	0	0	0	0	0	0	0	0	0	0	0	0	0	0	0	0	0
<i>Kyste Pentapharsodinium dalei</i>	0	0	0	5	0	2	0	0	0	1	0	2	4	0	0	0	2
<i>Islandinium minutum</i>	62	54	59	47	48	35	6	52	17	48	50	41	28	25	24	37	32
<i>Brigantedinium</i> spp.	18	18	13	13	18	33	4	9	6	23	29	11	22	13	13	14	8
<i>Brigantedinium cariacense</i>	0	0	0	0	0	0	0	0	0	0	0	0	1	1	0	1	0
<i>Brigantedinium simplex</i>	5	1	0	0	6	6	2	4	2	0	4	0	9	4	9	4	9
<i>Selenopemphix quanta</i>	0	0	0	0	0	0	0	0	0	0	0	0	0	0	1	5	3
<i>Trinoyantedinium applanatum</i>	0	0	0	0	0	0	0	0	0	0	0	0	0	0	0	0	1
Total	279	403	554	446	511	531	400	520	332	541	550	537	615	501	605	624	754
Concentration (dinokystes /cm³)	4414	3852	8199	16 156	10 604	13 209	29 149	11 503	4975	7285	7713	14 055	27 539	14 323	15 724	22 300	18 558

Tableau A.1. (suite)

Profondeur (cm)	17	18	19	20	21	22	23	24	25	26	27	28	29	30	31	32	33
<i>Ataxiodinium choane</i>	0	0	0	0	0	0	3	0	0	0	1	0	0	0	0	0	0
<i>Impagidinium pallidum</i>	5	2	1	1	0	0	3	1	0	0	0	0	0	0	1	0	0
<i>Impagidinium paradoxum</i>	0	0	0	0	0	0	0	0	0	0	0	0	0	0	0	0	0
<i>Impagidinium sphaericum</i>	0	1	1	0	1	0	0	0	0	0	0	0	0	2	2	1	0
<i>Nematosphaeropsis labyrinthus</i>	28	19	14	9	10	8	12	11	17	35	27	24	25	54	33	51	21
<i>Operculodinium centrocarpum</i>	557	553	514	431	348	262	301	307	340	161	231	404	206	348	366	381	177
<i>Operculodinium centrocarpum</i> court processus	20	9	5	4	3	18	10	24	15	22	9	28	27	29	27	22	13
<i>Spiniferites elongatus</i>	7	6	7	6	8	1	8	1	4	4	4	7	10	5	7	7	3
<i>Spiniferites ramosus</i>	13	12	7	3	1	2	3	7	4	1	3	2	4	3	7	4	1
<i>Spiniferites mirabilis-hyperacanthus</i>	3	1	2	1	1	2	0	0	1	0	1	0	0	0	0	2	0
<i>Spiniferites</i> spp.	0	0	0	0	0	0	0	0	0	0	0	0	0	1	0	0	0
Kyste <i>Pentapharsodinium dalei</i>	0	0	0	0	0	1	0	0	0	0	0	0	0	0	0	0	0
<i>Islandinium minutum</i>	20	27	42	30	38	31	35	25	29	22	18	42	38	2	3	10	9
<i>Brigantedinium</i> spp.	10	5	17	19	19	24	14	9	12	11	4	5	3	5	7	20	6
<i>Brigantedinium cariacense</i>	0	0	1	0	0	1	1	0	0	0	0	1	0	0	0	1	1
<i>Brigantedinium simplex</i>	12	13	13	9	14	16	7	6	6	7	5	4	5	2	1	9	3
<i>Selenopemphix quanta</i>	2	1	4	7	2	3	3	3	1	0	2	2	3	2	3	2	0
<i>Trinovantedinium app/lanatum</i>	1	1	0	0	0	0	0	0	1	0	0	0	0	0	0	0	1
Total	678	650	628	520	445	369	400	394	430	263	305	519	321	453	457	510	235
Concentration (dinokystes /cm³)	20 487	27 452	12 895	10 066	13 231	13 994	30 972	22 880	17 957	9309	13 495	19 484	8171	13 688	27 573	10 530	18 196

Tableau A.1. (suite)

Profondeur (cm)	34	35	36	37	38	39	40	41	42	43	44	45	46	47	48	49	50
<i>Ataxiodinium choane</i>	0	0	0	0	0	0	1	0	1	0	0	0	0	0	0	0	0
<i>Impagidinium pallidum</i>	1	0	0	1	0	0	1	3	0	0	0	0	0	0	0	0	0
<i>Impagidinium paradoxum</i>	0	1	0	0	0	0	0	0	0	0	0	0	0	0	0	0	0
<i>Impagidinium sphaericum</i>	1	2	2	3	3	1	4	1	1	0	1	1	0	0	0	0	1
<i>Nematosphaeropsis labyrinthus</i>	25	23	18	13	26	32	22	29	28	38	29	16	29	50	18	9	8
<i>Operculodinium centrocarpum</i>	256	291	308	303	307	170	207	300	594	436	471	415	524	436	360	327	303
<i>Operculodinium centrocarpum</i> court processus	13	13	39	25	42	30	50	38	43	41	27	61	62	59	24	50	49
<i>Spiniferites elongatus</i>	4	6	6	4	3	4	8	14	17	9	17	7	9	6	2	7	6
<i>Spiniferites ramosus</i>	0	4	1	5	2	3	0	2	4	0	5	2	0	3	1	4	0
<i>Spiniferites mirabilis-hyperacanthus</i>	0	0	0	1	2	0	3	2	3	1	4	2	0	2	0	0	1
<i>Spiniferites</i> spp.	1	1	1	0	0	0	1	0	0	0	0	0	1	0	0	2	0
<i>Kyste Pentapharsodinium dalei</i>	0	0	0	0	1	0	0	1	0	0	0	0	0	0	0	1	0
<i>Islandinium minutum</i>	46	50	15	12	18	7	27	18	18	11	5	14	10	40	30	30	24
<i>Brigantedinium</i> spp.	6	4	6	5	8	8	14	11	5	0	4	4	5	6	4	8	8
<i>Brigantedinium cariacense</i>	0	1	0	0	0	0	0	0	0	0	0	0	0	0	0	0	0
<i>Brigantedinium simplex</i>	2	4	7	3	4	1	7	6	1	1	0	3	0	2	1	5	2
<i>Selenopemphix quanta</i>	0	1	0	1	1	0	1	0	1	0	1	0	0	1	0	1	1
<i>Trinovantedinium applanatum</i>	0	0	0	0	0	0	0	0	1	0	0	0	0	0	0	0	0
Total	355	401	403	376	417	256	346	425	717	537	564	525	640	605	440	444	403
Concentration (dinokystes /cm³)	9371	13 427	13 616	14 866	11 922	11 893	7391	11 046	20 657	23 760	34 936	20 325	26 139	38 111	36 340	15 279	8368

Tableau A.2.
Dénombrements et concentrations des grains de pollen et des spores de la carotte JM-06-WP-04-MCB

Profondeur (cm)	0	1	2	3	4	5	6	7	8	9	10	11	12	13	14	15	16
<i>Abies</i>	0	0	0	0	0	0	0	0	0	0	0	0	0	0	0	0	0
<i>Picea</i>	0	0	0	0	0	0	0	0	0	0	0	0	0	0	0	0	0
<i>Pinus</i>	9	4	2	2	5	7	1	2	1	6	6	1	1	2	3	1	1
<i>Corylus</i>	0	0	1	0	0	0	0	0	0	0	0	0	0	0	0	0	0
<i>Juniperus</i>	1	0	0	0	0	0	0	0	0	0	0	0	0	0	0	0	0
<i>Betula</i>	0	0	0	0	1	0	0	0	0	0	0	0	0	0	0	0	0
<i>Alnus</i> spp.	0	3	0	0	0	0	0	0	0	0	0	0	0	0	0	0	0
<i>Alnus</i> type <i>crispa</i>	1	0	0	0	0	0	0	0	0	0	0	0	0	0	0	0	0
<i>Alnus</i> type <i>rugosa</i>	0	0	0	0	0	0	0	0	0	0	0	0	0	0	0	0	0
Indéterminés	0	1	0	0	0	0	0	0	0	0	0	0	0	0	1	0	0
<i>Lycopodium annotinum</i>	1	5	3	0	1	0	0	0	0	0	0	0	0	0	0	0	0
<i>Lycopodium clavatum</i>	0	0	0	0	1	0	0	0	0	0	0	0	0	0	0	0	0
Spore monolète	1	0	0	0	0	0	0	0	0	0	0	0	0	0	0	0	0
Spore trilète	4	5	5	4	6	6	3	2	4	2	6	2	2	1	1	1	4
<i>Sphagnum</i>	4	5	2	1	0	1	1	0	0	0	0	0	1	0	6	2	2
Total	21	23	13	7	14	14	5	4	5	8	12	3	4	3	11	4	7
Concentration (pollens / cm³)	174	77	44	72	125	174	73	44	15	81	84	26	45	57	78	36	25
Concentration (spores / cm³)	158	143	148	181	166	174	291	44	59	26	84	52	134	29	208	107	148

Tableau A.2. (suite)

Profondeur (cm)	17	18	19	20	21	22	23	24	25	26	27	28	29	30	31	32	33
<i>Abies</i>	0	0	0	0	0	0	0	0	0	0	0	0	0	0	0	0	0
<i>Picea</i>	0	0	0	0	0	0	0	0	0	0	0	0	0	0	0	0	0
<i>Pinus</i>	3	3	3	9	4	0	4	2	2	0	2	4	5	11	3	7	2
<i>Corylus</i>	0	0	0	0	0	0	0	0	0	0	0	0	0	0	0	0	0
<i>Juniperus</i>	0	0	0	0	0	0	0	0	0	0	0	0	0	0	0	0	0
<i>Betula</i>	0	0	0	0	0	0	0	0	0	0	0	0	0	0	0	0	0
<i>Alnus</i> spp.	0	0	0	0	0	0	0	0	0	0	0	0	0	0	0	0	0
<i>Alnus</i> type <i>crispa</i>	0	0	0	0	0	0	0	0	0	0	0	0	0	0	0	0	0
<i>Alnus</i> type <i>rugosa</i>	0	0	0	0	0	0	0	0	0	0	0	0	0	0	0	0	0
Indéterminés	0	0	0	0	0	0	0	0	0	0	0	0	0	0	0	0	0
<i>Lycopodium annotinum</i>	0	0	0	0	0	0	2	0	0	0	0	0	1	2	0	3	0
<i>Lycopodium clavatum</i>	0	0	0	0	0	0	0	0	0	0	0	0	0	0	0	0	0
Spore monolète	0	0	0	0	0	0	0	0	1	0	0	0	0	0	0	0	0
Spore trilète	2	1	0	1	3	1	0	0	0	1	1	1	0	0	2	0	0
<i>Sphagnum</i>	0	1	4	0	1	1	2	0	0	1	1	2	2	2	1	1	0
Total	5	5	7	10	8	2	8	2	3	2	4	7	8	15	6	11	2
Concentration (pollens / cm³)	91	127	62	174	119	0	310	116	83	0	89	150	127	363	181	144	155
Concentration (spores / cm³)	60	84	82	19	119	76	310	0	42	71	133	113	76	121	181	62	0

Tableau A.2. (suite)

Profondeur (cm)	34	35	36	37	38	39	40	41	42	43	44	45	46	47	48	49	50
<i>Abies</i>	0	0	0	0	0	1	0	0	0	0	0	0	0	0	0	0	0
<i>Picea</i>	0	0	0	0	0	0	2	1	1	0	2	1	0	1	0	0	0
<i>Pinus</i>	1	2	6	5	2	3	6	4	3	4	4	3	2	4	3	3	4
<i>Corylus</i>	0	0	0	0	0	0	3	0	0	0	0	0	0	0	1	0	1
<i>Juniperus</i>	0	0	0	0	0	0	0	0	0	0	0	0	0	0	0	0	0
<i>Betula</i>	0	0	0	0	0	0	2	0	0	0	0	0	0	0	0	3	0
<i>Alnus</i> spp.	0	0	0	0	0	0	1	0	0	0	0	0	0	0	0	0	0
<i>Alnus</i> type <i>crispa</i>	0	0	0	0	0	0	0	0	0	0	0	0	0	0	0	0	0
<i>Alnus</i> type <i>rugosa</i>	0	0	0	0	0	0	0	1	0	0	0	0	0	0	0	0	0
Indéterminés	0	0	0	0	0	0	0	0	0	0	0	0	0	0	0	0	0
<i>Lycopodium annotinum</i>	0	0	1	3	5	0	2	3	3	2	3	1	2	2	2	1	3
<i>Lycopodium clavatum</i>	0	0	0	0	0	0	0	0	0	0	0	0	0	0	0	0	0
Spore monolète	0	0	0	0	0	0	0	0	0	0	0	0	0	0	0	0	0
Spore trilète	0	1	0	0	0	0	0	0	0	3	3	3	1	0	0	0	0
<i>Sphagnum</i>	2	0	3	1	2	1	2	0	1	1	2	1	3	2	0	3	2
Total	3	3	10	9	9	5	18	9	8	10	14	9	8	9	6	10	10
Concentration (pollens / cm³)	26	100	270	198	172	186	299	156	115	177	372	155	82	315	330	206	104
Concentration (spores / cm³)	53	34	135	158	200	46	85	78	86	265	496	194	245	252	165	138	104

Tableau A.3.
Dénombrements et concentrations des palynomorphes remaniés* et des réseaux organiques
de foraminifères benthiques de la carotte JM-06-WP-04-MCB

Profondeur (cm)	0	1	2	3	4	5	6	7	8	9	10	11	12	13	14	15	16
Nombre de remaniés	2	6	8	1	1	0	2	3	2	2	2	0	8	10	5	1	7
Concentration (remaniés / cm ³)	32	57	118	36	21	0	146	66	30	27	28	0	358	286	130	36	172
Nombre de réseaux organiques	30	76	91	75	69	48	0	12	41	33	85	22	75	27	80	35	119
Concentration (réseaux organiques /cm ³)	475	726	1347	2717	1432	1194	0	265	614	444	1192	576	3358	772	2079	1251	2929
Profondeur (cm)	17	18	19	20	21	22	23	24	25	26	27	28	29	30	31	32	33
Nombre de remaniés	4	1	4	1	3	3	1	0	1	3	0	5	6	7	3	7	5
Concentration (remaniés / cm ³)	120	42	82	19	89	114	77	0	42	106	0	188	153	211	181	145	387
Nombre de réseaux organiques	161	97	199	174	141	102	69	39	62	21	36	60	60	54	24	101	25
Concentration (réseaux organiques /cm ³)	4865	4097	4086	3368	4192	3868	5343	2265	2589	743	1593	2252	1527	1632	1448	2085	1936
Profondeur (cm)	34	35	36	37	38	39	40	41	42	43	44	45	46	47	48	49	50
Nombre de remaniés	4	12	12	10	11	4	12	10	7	0	1	4	2	2	0	0	5
Concentration (remaniés / cm ³)	106	402	405	395	315	186	256	260	202	0	62	155	82	126	0	0	104
Nombre de réseaux organiques	43	48	149	117	82	93	164	135	69	42	47	63	56	37	52	43	82
Concentration (réseaux organiques /cm ³)	1135	1607	5034	4626	2344	4321	3503	3509	1988	1858	2911	2439	2287	2331	4295	1480	1703

* Les palynomorphes incluent tous les microfossiles à paroi organique (composée de chitine et de sporopollénine), d'origine continentale et marine. Les remaniés incluent les organismes pré-Quaternaires et ceux qui ne peuvent être identifiés en raison d'un mauvais état de conservation (gymnospermes, spores trilètes, triporés, acritarches, dinokystes).

APPENDICE B

TABLEAUX DE COMPTAGES ET CONCENTRATIONS DES PALYNOMORPHES TERRESTRES ET MARINS DES ÉCHANTILLONS DE SURFACE DES MERS NORDIQUES (PROFONDEUR: 0-1 CM)

Tableau B.1. Dénombrements et concentrations des dinokystes des échantillons de surface des mers nordiques (profondeur : 0-1 cm).....64

Tableau B.2. Dénombrements et concentrations des grains de pollen et des spores des échantillons des mers nordiques (profondeur : 0-1 cm).....66

Tableau B.3. Dénombrements et concentrations des palynomorphes remaniés et des réseaux organiques de foraminifères benthiques des échantillons de surface des mers nordiques (profondeur : 0-1 cm).....68

Tableau B.1.

Dénombrements et concentrations des dinokystes des échantillons de surface des mers nordiques (profondeur : 0-1 cm)

Carotte	HLY0503-22MC-8	JM06-WP-7-BCC	JM06-WP-04-MCB	JM06-WP-10-BCB	JM06-WP-12-BCB	JM06-WP-14-BCE	JM06-WP-16-MCB	JM06-WP-19-MCB	JM06-WP-21-MCE	JM06-WP-26-MCC
<i>Ataxiodinium choane</i>	0	1	0	0	0	0	0	0	0	0
<i>Blechnodinium lepticiense</i>	0	1	0	0	0	6	0	0	0	0
<i>Impagidinium pallidum</i>	11	0	0	6	2	7	2	2	1	1
<i>Impagidinium sphaericum</i>	1	0	0	0	0	1	0	0	0	0
<i>Nematosphaeropsis labyrinthus</i>	22	10	13	35	16	35	27	8	8	1
<i>Operculodinium centrocarpum</i>	276	109	169	482	230	366	271	84	105	49
<i>Operculodinium centrocarpum</i> oost processus	6	5	1	14	9	13	3	4	6	4
<i>Spiniferites elongatus</i>	6	1	4	18	0	8	8	3	3	0
<i>Spiniferites ramosus</i>	2	1	7	5	0	1	1	0	0	0
<i>Spiniferites mirabilis-hyperacanthus</i>	0	0	0	2	0	0	0	0	0	0
<i>Spiniferites</i> spp.	2	0	0	0	0	1	2	0	0	0
<i>Kystis Pentapharsodinium dalei</i>	18	1	0	2	0	5	0	0	1	1
<i>Islandinium minusculum</i>	23	32	62	24	25	48	13	33	16	13
<i>Islandinium?</i> cesare	5	0	0	0	0	0	0	0	0	0
<i>Brigantedinium</i> spp.	9	25	18	6	7	18	3	18	7	0
<i>Brigantedinium cartacoense</i>	0	0	0	0	0	0	0	2	0	0
<i>Brigantedinium simplex</i>	0	4	5	2	1	4	6	3	2	0
<i>Selenopemphix quanta</i>	0	0	0	0	0	0	1	0	0	0
<i>Trinovantidium applanatum</i>	0	0	0	1	0	0	0	0	0	0
Total	381	190	279	597	290	513	337	157	149	69
Concentration (dinokystes /cm³)	27 985	2278	4414	14 792	3849	3351	6231	994	1191	629

Tableau B.1. (suite)

Carotte	JM06-WP-24-MCA	JM07-WP-168-MCB	JM07-WP-170-MCB	JM07-WP-171-MCB	JM07-WP-172-MCB	JM07-WP-176-MCB	JM07-WP-180-MCB	JM07-WP-182-MCB	JM07-WP-183-MCB
<i>Ataxiodinium choan</i>	0	0	0	0	0	0	0	0	0
<i>Blectatodinium tepikiense</i>	0	0	0	0	0	0	0	0	0
<i>Impagidinium pallidum</i>	2	11	8	37	19	7	11	18	2
<i>Impagidinium sphaericum</i>	0	0	0	0	0	0	0	0	0
<i>Nematosphaeropsis labyrinthus</i>	14	4	21	21	18	2	10	24	3
<i>Operculodinium centrocarpum</i>	47	8	114	101	110	5	29	79	19
<i>Operculodinium centrocarpum</i> court processus	3	0	15	5	5	0	1	6	5
<i>Spiniferites elongatus</i>	0	0	7	3	1	0	0	4	2
<i>Spiniferites ramosus</i>	0	0	0	1	0	0	0	0	0
<i>Spiniferites mirabilis-hyperacanthus</i>	0	0	0	0	0	0	0	0	0
<i>Spiniferites</i> spp.	0	0	0	2	0	0	0	1	0
<i>Kyste Pentapharsodinium dalei</i>	0	0	1	4	1	0	1	0	1
<i>Islandinium minutum</i>	19	1	39	21	33	258	18	18	163
<i>Islandinium? cesare</i>	0	0	2	3	5	0	0	2	0
<i>Brigantedinium</i> spp.	6	8	19	13	14	35	6	10	16
<i>Brigantedinium carliacoense</i>	0	0	0	0	0	0	0	0	0
<i>Brigantedinium simplex</i>	1	0	0	2	4	9	0	2	0
<i>Selenopemphix quania</i>	0	0	0	0	0	0	0	0	1
<i>Trinovantedinium applanatum</i>	0	0	0	0	0	0	0	0	0
Total	92	32	226	213	210	316	76	164	212
Concentration (dinokystes /cm ³)	756	196	1795	1706	1555	4432	1127	1071	13 585

Tableau B.2.
Dénombrements et concentrations des grains de pollen et des spores des échantillons des mers nordiques
(profondeur : 0-1 cm)

Carotte	HL0503-22MC-8	JM06-WP-7-BCC	JM06-WP-04-MCB	JM06-WP-10-BCB	JM06-WP-12-BCB	JM06-WP-14-BCE	JM06-WP-16-MCB	JM06-WP-19-MCB	JM06-WP-21-MCE	JM06-WP-26-MCC
<i>Abies</i>	0	0	0	0	0	1	0	0	0	0
<i>Picea</i>	1	3	0	2	3	3	0	4	1	0
<i>Pinus</i>	5	6	9	4	3	7	3	6	4	0
<i>Corylus</i>	0	0	0	0	0	0	0	0	0	0
<i>Juniperus</i>	0	0	1	0	0	0	0	0	0	0
<i>Betula</i>	1	1	0	0	0	1	1	2	0	0
<i>Alnus</i> spp.	0	0	0	1	0	0	0	1	0	0
<i>Alnus type crispa</i>	0	0	1	0	0	0	0	0	0	0
<i>Lycopodium annotinum</i>	0	1	1	0	2	1	1	1	0	1
<i>Lycopodium clavatum</i>	0	0	0	1	0	0	2	0	0	1
Spore monolète	0	0	1	0	0	0	0	0	0	0
Spore trilète	17	1	4	1	1	1	0	0	2	1
<i>Sphagnum</i>	3	12	4	0	3	2	0	4	1	1
<i>Osmonda</i>	0	0	0	0	1	0	0	0	0	0
Total	27	24	21	9	13	16	7	18	8	4
Concentration (pollens / cm ³)	514	120	174	173	80	78	74	82	40	0
Concentration (spores / cm ³)	1469	168	158	50	93	26	55	32	24	36

Tableau B.2. (suite)

Carotte	JM06-WP-24-MCA	JM07-WP-168-MCB	JM07-WP-170-MCB	JM07-WP-171-MCB	JM07-WP-172-MCB	JM07-WP-176-MCB	JM07-WP-180-MCB	JM07-WP-182-MCB	JM07-WP-183-MCB
<i>Abies</i>	0	0	0	0	0	0	0	0	0
<i>Picea</i>	3	0	1	1	0	0	0	0	0
<i>Pinus</i>	6	3	7	7	13	1	4	8	1
<i>Corylus</i>	1	0	0	0	0	0	0	0	0
<i>Juniperus</i>	0	0	0	0	0	0	0	0	0
<i>Betula</i>	0	1	0	0	3	0	0	2	0
<i>Alnus</i> spp.	0	0	0	0	0	0	0	0	0
<i>Alnus</i> type <i>crispa</i>	0	0	0	0	0	0	0	0	0
<i>Lycopodium annotinum</i>	0	3	1	0	0	0	0	0	0
<i>Lycopodium clavatum</i>	0	0	0	0	0	0	0	0	0
Spore monolète	0	0	0	0	0	0	0	0	0
Spore trilète	1	0	1	0	0	0	0	0	0
<i>Sphagnum</i>	0	0	3	0	4	1	1	0	1
<i>Osmonda</i>	0	0	0	0	0	0	0	0	0
Total	11	7	13	8	20	2	5	10	2
Concentration (pollens / cm³)	82	24	63	64	118	14	59	65	64
Concentration (spores / cm³)	8	18	40	0	30	14	15	0	64

Tableau B.3.

Dénombrements et concentrations des palynomorphes remaniés* et des réseaux organiques de foraminifères benthiques des échantillons de surface des mers nordiques (profondeur : 0-1 cm)

Nom de la carotte	Profondeur (cm)	Nombre de remaniés	Concentration (remaniés / cm ³)	Nombre de réseaux organiques	Concentration (réseaux organiques / cm ³)
HLY0503-22MC-8	0-1	3	220	53	3893
JM06-WP-7-BCC	0-1	7	84	135	1619
JM06-WP-04-MCB	0-1	2	32	30	475
JM06-WP-10-BCB	0-1	5	124	147	3642
JM06-WP-12-BCB	0-1	6	80	198	2628
JM06-WP-14-BCE	0-1	5	33	356	2325
JM06-WP-16-MCB	0-1	0	0	552	10 207
JM06-WP-19-MCB	0-1	4	25	549	3476
JM06-WP-21-MCE	0-1	2	16	148	1183
JM06-WP-26-MCC	0-1	1	9	161	1467
JM06-WP-24-MCA	0-1	0	0	277	2278
JM07-WP-168-MCB	0-1	1	6	52	318
JM07-WP-170-MCB	0-1	0	0	280	2224
JM07-WP-171-MCB	0-1	1	8	118	945
JM07-WP-172-MCB	0-1	6	44	329	2436
JM07-WP-176-MCB	0-1	2	28	111	1557
JM07-WP-180-MCB	0-1	1	15	416	6170
JM07-WP-182-MCB	0-1	1	6	698	4559
JM07-WP-183-MCB	0-1	2	128	75	4806

* Les palynomorphes incluent tous les microfossiles à paroi organique (composée de chitine et de sporopllénine), d'origine continentale et marine. Les remaniés incluent les organismes pré-Quaternaires et ceux qui ne peuvent être identifiés en raison d'un mauvais état de conservation (gymnospermes, spores trilètes, triporés, acritarches, dinokystes).

BIBLIOGRAPHIE GÉNÉRALE

- ACSYS, 2003. ACSYS Historical Ice Chart Archive (1553-2002), IACPO Informal Report 8. Digital Media, Arctic Climate System Study, Norwegian Polar Institute, Tromsø, Norway.
- Addinsoft, 2008. XLSTAT 2008, Data Analysis and Statistics Software for Microsoft Excel. Paris, France.
- Alley, R.B., Mayewski, P.A., Sowers, T., Stuiver, M., Taylor, K.C. et Clark, P.U., 1997. Holocene climatic instability; a prominent, widespread event 8200 yr ago. *Geology* 25(6), 483-486.
- Andersson, C., Risebrobakken, B., Jansen, E. et Dahl, S.O., 2003. Late Holocene surface ocean conditions of the Norwegian Sea (Voring Plateau). *Paleoceanography* 18(2), PA1044. doi: 10.1029/2001PA000654.
- Bendle, J.A.P. et Rosell-Mele, A., 2007. High-resolution alkenone sea surface temperature variability on the North Icelandic Shelf: implications for Nordic Seas palaeoclimatic development during the Holocene. *The Holocene* 17(1), 9-24.
- Bennike, O., 2004. Holocene sea-ice variations in Greenland: onshore evidence. *The Holocene* 14(4), 607.
- Berger, W.H. et Johnson, R.F., 1978. On the thickness and the ^{14}C age of the mixed layer in deep-sea carbonates. *Earth and Planetary Science Letters* 41(2).
- Bianchi, G.G. et McCave, I.N., 1999. Holocene periodicity in North Atlantic climate and deep-ocean flow south of Iceland. *Nature* 397(6719), 515-517.
- Bond, G., Showers, W., Cheseby, M., Lotti, R., Almasi, P., deMenocal, P., Priore, P., Cullen, H., Hajdas, I. et Bonani, G., 1997. A Pervasive Millennial-Scale Cycle in North Atlantic Holocene and Glacial Climates. *Science* 278(5341), 1257.
- Bond, G.C., Showers, W., Elliot, M., Evans, M., Lotti, R., Hajdas, I., Bonani, G. et Johnson, S., 1999. The North Atlantic's 1-2 kyr Climate Rhythm: Relation to Heinrich Events, Dansgaard/Oeschger Cycles and the Little Ice Age. *Geophysical Monograph-American Geophysical Union* 112 35-58.

- Bond, G., Kromer, B., Beer, J., Muscheler, R., Evans, M.N., Showers, W., Hoffmann, S., Lotti-Bond, R., Hajdas, I. et Bonani, G., 2001. Persistent Solar Influence on North Atlantic Climate During the Holocene. *Science* 294(5549), 2130-2136.
- Bonnet, S., 2009. Variability of sea-surface temperature and sea-ice cover in the Fram Strait over the last two millennia M.Sc. Thesis, Université du Québec à Montréal, Montréal, Québec, Canada.
- Calvo, E., Grimalt, J. et Jansen, E., 2002. High resolution UK37 sea surface temperature reconstruction in the Norwegian Sea during the Holocene. *Quaternary Science Reviews* 21(12-13), 1385-1394.
- Campbell, I.D., Campbell, C., Apps, M.J., Rutter, N.W. et Bush, A.B.G., 1998. Late Holocene approximately 1500 yr climatic periodicities and their implications. *Geology* 26(5), 471-473.
- Dahl, S.O. et Nesje, A., 1994. Holocene glacier fluctuations at Hardangerjokulen, central-southern Norway: a high-resolution composite chronology from lacustrine and terrestrial deposits. *The Holocene* 4(3), 269.
- Darby, D., 2005. CRUISE REPORT HLY0503: Healy-Oden Trans-Arctic Expedition. Department of Ocean, Earth and Atmospheric Sciences, Old Dominion University, USA.
- de Vernal, A., et Marret, F., 2007. Organic-walled dinoflagellate cysts: tracers of sea-surface conditions. In: Hillaire-Marcel, C., de Vernal, A. (Eds.), *Proxies in Late Cenozoic paleoceanography*. Developments in Marine Geology, Elsevier, pp. 371-408.
- de Vernal, A., Larouche, A. et Richard, P.J.H., 1987. Evaluation of palynomorph concentrations: do the aliquot and the marker-grain methods yield comparable results? *Pollen et spores* 29(2-3), 291-303.
- de Vernal, A., Turon, J.L. et Guiot, J., 1994. Dinoflagellate cyst distribution in high-latitude marine environments and quantitative reconstruction of sea-surface salinity, temperature, and seasonality. *Canadian Journal of Earth Sciences* 31(1), 48-62.
- de Vernal, A., Henry, M., et Bilodeau, G., 1996. Technique de préparation et d'analyse en Micropaléontologie, Les cahiers du GEOTOP 3, unpublished report, Université du Québec à Montréal, Montréal, Québec, Canada.

- de Vernal, A., Rochon, A., Turon, J.L. et Matthiessen, J., 1997. Organic-walled dinoflagellate cysts: Palynological tracers of sea-surface conditions in middle to high latitude marine environments. *Geobios(Lyon)* 30(7), 905-920.
- de Vernal, A., Henry, M., Matthiessen, J., Mudie, P.J., Rochon, A., Boessenkool, K.P., Eynaud, F., Grosfjeld, K., Guiot, J. et Hamel, D., 2001. Dinoflagellate cyst assemblages as tracers of sea-surface conditions in the northern North Atlantic, Arctic and sub-Arctic seas: the new "n= 677" data base and its application for quantitative paleoceanographic reconstruction. *Journal of Quaternary Science* 16(7), 681-698.
- de Vernal, A., Eynaud, F., Henry, M., Hillaire-Marcel, C., Londeix, L., Mangin, S., Matthiessen, J., Marret, F., Radi, T. et Rochon, A., 2005. Reconstruction of sea-surface conditions at middle to high latitudes of the Northern Hemisphere during the Last Glacial Maximum (LGM) based on dinoflagellate cyst assemblages. *Quaternary Science Reviews* 24(7-9), 897-924.
- Dickson, R., Rudels, B., Dye, S., Karcher, M., Meincke, J. et Yashayaev, I., 2007. Current estimates of freshwater flux through Arctic and subarctic seas. *Progress in Oceanography* 73(3-4), 210-230.
- Eiriksson, J., Bartels-Jonsdottir, H.B., Cage, A.G., Gudmundsdottir, E.R., Klitgaard-Kristensen, D., Marret, F., Rodrigues, T., Abrantes, F., Austin, W.E.N. et Jiang, H., 2006. Variability of the North Atlantic Current during the last 2000 years based on shelf bottom water and sea surface temperatures along an open ocean/shallow marine transect in western Europe. *The Holocene* 16(7), 1017-1029.
- Fahrbach, E., Meincke, J., Osterhus, S., Rohardt, G., Schauer, U., Tverberg, V. et Verduin, J., 2001. Direct measurements of volume transports through Fram Strait. *Polar Research* 20(2), 217-224.
- GIEC, 2007. Bilan 2007 des changements climatiques. Contribution des Groupes de travail I, II et III au quatrième Rapport d'évaluation du Groupe d'experts intergouvernemental sur l'évolution du climat [Équipe de rédaction principale, Pachauri, R.K. et Reisinger, A. (publié sous la direction de~)]. GIEC, Genève, Suisse.
- Grudd, H., Briffa, K.R., Karlen, W., Bartholin, T.S., Jones, P.D., et Kromer, B., 2002. A 7400-year tree-ring chronology in northern Swedish Lapland: natural climatic variability expressed on annual to millennial timescales. *The Holocene*, 12(6), 657-665.

- Guiot, J., 1990. Methodology of palaeoclimatic reconstruction from pollen in France. *Palaeogeography, Palaeoclimatology, Palaeoecology* 80, 49-69.
- Guiot, J. et Goeury, C., 1996. PPPBASE, a software for statistical analysis of paleoecological and paleoclimatological data. *Dendrochronologia* 14, 295-300.
- Guiot, J. et de Vernal, A., 2007. Transfer functions: methods for quantitative paleoceanography based on microfossils. In: Hillaire-Marcel, C., de Vernal, A. (Eds.), *Proxies in Late Cenozoic paleoceanography*. Developments in Marine Geology, Elsevier, pp. 523-563.
- Hald, M., Ebbesen, H., Forwick, M., Godtliebsen, F., Khomenko, L., Korsun, S., Ringstad Olsen, L. et Vorren, T.O., 2004. Holocene paleoceanography and glacial history of the West Spitsbergen area, Euro-Arctic margin. *Quaternary Science Reviews* 23(20-22), 2075-2088.
- Hald, M., Andersson, C., Ebbesen, H., Jansen, E., Klitgaard-Kristensen, D., Risebrobakken, B., Salomonsen, G.R., Sarnthein, M., Sejrup, H.P. et Telford, R.J., 2007. Variations in temperature and extent of Atlantic Water in the northern North Atlantic during the Holocene. *Quaternary Science Reviews* 26, 3423-3440.
- Hansen, B. et Østerhus, S., 2000. North Atlantic–Nordic Seas exchanges. *Progress in Oceanography* 45(2), 109-208.
- Head, M.J., Harland, R. et Matthiessen, J., 2001. Cold marine indicators of the late Quaternary: the new dinoflagellate cyst genus *Islandinium* and related morphotypes. *Journal of Quaternary Science* 16(7), 621-636.
- Holfort, J. et Meincke, J., 2005. Time series of freshwater-transport on the East Greenland Shelf at 74N. *Meteorologische Zeitschrift* 14(6), 703-710.
- Hughen, K.A., Baillie, M.G.L., Bard, E., Beck, J.W., Bertrand, C.J.H., Blackwell, P.G., Buck, C.E., Burr, G.S., Cutler, K.B. et Damon, P.E., 2004. Marine04 Marine Radiocarbon Age Calibration, 026 Cal Kyr BP. *Radiocarbon* 46(3), 1059-1086.
- Husum, K., 2006. CRUISE REPORT JM06-WP: Marine geological cruise to West Spitsbergen Margin and Fram Strait. Department of Geology, University of Tromsø, Norway.

- Husum, K., 2007. CRUISE REPORT JM07-WP: Marine geological cruise to East Greenland Margin. Department of Geology, University of Tromsø, Norway.
- Husum, K. et Hald, M., 2004. A continuous marine record 8000-1600 cal. yr BP from the Malangenfjord, north Norway: foraminiferal and isotopic evidence. *The Holocene* 14(6), 877-887.
- IPCC, 2007. Climate Change 2007: The Physical Science Basis. Contribution of Working Group I to the Fourth Assessment Report of the Intergovernmental Panel on Climate Change [Solomon, S., D. Qin, M. Manning, Z. Chen, M. Marquis, K.B. Averyt, M. Tignor and H.L. Miller (eds.)]. Cambridge University Press, Cambridge, United Kingdom and New York, NY, USA. IPCC, Genève, Suisse.
- Jennings, A.E. et N.J. Weiner. 1996. Environmental change in eastern Greenland during the last 1300 years: evidence from foraminifera and lithofacies in Nansen Fjord, 68°N. *The Holocene*, 6(2), 179-191.
- Jiang, H., Seidenkrantz, M.S., Knudsen, K.L. et Eriksson, J., 2002. Late-Holocene summer sea-surface temperatures based on a diatom record from the north Icelandic shelf. *The Holocene* 12(2), 137-147.
- Karlén, W. et Kuylenstierna, J., 1996. On solar forcing of Holocene climate: evidence from Scandinavia. *The Holocene* 6(3), 359-365.
- Koenigk, T., Mikolajewicz, U., Haak, H. et Jungclaus, J., 2006. Variability of Fram Strait sea ice export: causes, impacts and feedbacks in a coupled climate model. *Climate Dynamics* 26(1), 17-34.
- Kokinos, J.P., Eglinton, T., Goni, M.A., Boon, J.J., Martoglio, P.A et Anderson, D.M., 1998. Characterization of a highly resistant biomacromolecular material in the cell wall of a marine dinoflagellate resting cyst. *Organic geochemistry*, 28, 265-288.
- Komuro, Y. et Hasumi, H., 2007. Effects of variability of sea ice transport through the Fram Strait on the intensity of the Atlantic deep circulation. *Climate Dynamics* 29(5), 455-467.
- Krauss, W., Fahrbach, E., Aitsam, A., Elken, J. et Koshe, P., 1987. The North Atlantic current and its associated eddy field southeast of Flemish Cap. *Deep-sea research. Part A. Oceanographic research papers* 34(7), 1163-1185.

- Kucera, M., Weinelt, M., Kiefer, T., Pflaumann, U., Hayes, A., Weinelt, M., Chen, M.T., Mix, A.C., Barrows, T.T. et Cortijo, E., 2005. Reconstruction of sea-surface temperatures from assemblages of planktonic foraminifera: multi-technique approach based on geographically constrained calibration data sets and its application to glacial Atlantic and Pacific Oceans. *Quaternary Science Reviews* 24(7-9), 951-998.
- MacDonald, G.M., Velichko, A.A., Kremenetski, C.V., Borisova, O.K., Goleva, A.A., Andreev, A.A., Cwynar, L.C., Riding, R.T., Forman, S.L. et Edwards, T.W.D., 2000. Holocene Treeline History and Climate Change Across Northern Eurasia. *Quaternary Research* 53(3), 302-311.
- Malmgren, B.A. et Nordlund, U., 1997. Application of artificial neural networks to paleoceanographic data. *Palaeogeography, Palaeoclimatology, Palaeoecology* 136(1), 359-373.
- Matthews, J., 1969. The assessment of a method for the determination of absolute pollen frequencies. *New Phytologist* 68(1), 161-166.
- McDermott, F., Matthey, D.P., et Hawkesworth, C., 2001. Centennial-scale Holocene climate variability revealed by a high-resolution speleothem $\delta^{18}\text{O}$ record from SW Ireland. *Science* 294, 1328-1331.
- Mikalsen, G., Sejrup, H.P., et Aarseth, I., 2001. Late-Holocene changes in ocean circulation and climate: foraminiferal and isotopic evidence from Sulafjord, western Norway. *The Holocene*, 11(4), 437-446.
- Mudie, P.J. et Rochon, A., 2001. Distribution of dinoflagellate cysts in the Canadian Arctic marine region. *Journal of Quaternary Science* 16(7), 603-620.
- Nesje, A., Matthews, J.A., Dahl, S.O., Berrisford, M.S. et Andersson, C., 2001. Holocene glacier fluctuations of Flatebreen and winter-precipitation changes in the Jostedalsbreen region, western Norway, based on glaciolacustrine sediment records. *The Holocene* 11(3), 267-280.
- NODC (National Oceanographic Data Center), 2001. World Ocean Database 2001, Scientific Data Sets, Observed and Standard Level Oceanographic Data [CD-Rom], National Oceanic and Atmospheric Administration.
- NSIDC (National Snow and Ice Data Center), 2003. Brightness temperature and ice concentrations grids for the polar regions. User's guide. NSIDC Distributed Active Archive Center, University of Colorado, Boulder.

- O'Brien, S.R., Mayewski, P.A., Meeker, L.D., Meese, D.A., Twickler, M.S. et Whitlow, S.I., 1995. Complexity of Holocene Climate as Reconstructed from a Greenland Ice Core. *Science* 270(5244), 1962-1964.
- Peyron, O. et de Vernal, A., 2001. Application of artificial neural networks (ANN) to high latitude dinocyst assemblages for the reconstruction of past sea-surface conditions in Arctic and sub-Arctic seas. *Journal of Quaternary Science* 16(7), 699-709.
- Risebrobakken, B., Jansen, E., Andersson, C., Mjelde, E. et Hevrøy, K., 2003. A high-resolution study of Holocene paleoclimatic and paleoceanographic changes in the Nordic Seas. *Paleoceanography* 18(1), PA1017. doi: 10.1029/2002PA000764.
- Rochon, A., de Vernal, A., Turon, J.-L., Matthiessen, J. et Head, M.J., 1999. Distribution of Recent Dinoflagellate Cysts in Surface Sediments from the North Atlantic Ocean and Adjacent Seas in Relation to Sea-surface Parameters. *American Association of Stratigraphic Palynologists Foundation*.
- Rousse, S., Kissel, C., Laj, C., Eiríksson, J. et Knudsen, K.L., 2006. Holocene centennial to millennial-scale climatic variability: Evidence from high-resolution magnetic analyses of the last 10 cal kyr off North Iceland (core MD99-2275). *Earth and Planetary Science Letters* 242(3-4), 390-405.
- Rudels, B., Björk, G., Nilsson, J., Winsor, P., Lake, I. et Nohr, C., 2005. The interaction between waters from the Arctic Ocean and the Nordic Seas north of Fram Strait and along the East Greenland Current: results from the Arctic Ocean-02 Oden expedition. *Journal of Marine Systems* 55(1-2), 1-30.
- Sarnthein, M., Kreveld, S., Erlenkeuser, H., Grootes, P.M., Kucera, M., Pflaumann, U. et Schulz, M., 2003. Centennial-to-millennial-scale periodicities of Holocene climate and sediment injections off the western Barents shelf, 75° N. *Boreas* 32(3), 447-461.
- Schauer, U., Loeng, H., Rudels, B., Ozhigin, V.K. et Dieck, W., 2002. Atlantic Water flow through the Barents and Kara Seas. *Deep-Sea Research Part I* 49(12), 2281-2298.
- Seppä, H. et Birks, H.J.B., 2002. Holocene Climate Reconstructions from the Fennoscandian Tree-Line Area Based on Pollen Data from Toskaljavri. *Quaternary Research* 57(2), 191-199.

- Ślubowska-Woldengen, M.A., Rasmussen, T.L., Koç, N., Klitgaard-Kristensen, D., Nilsen, F. et Solheim, A., 2007. Advection of Atlantic Water to the western and northern Svalbard shelves through the last 17.5 ka cal yr BP. *Quaternary Science Reviews* 26, 463-478.
- Solignac, S., de Vernal, A. et Hillaire-Marcel, C., 2004. Holocene sea-surface conditions in the North Atlantic—contrasted trends and regimes in the western and eastern sectors (Labrador Sea vs. Iceland Basin). *Quaternary Science Reviews* 23(3-4), 319-334.
- Stuiver, M., Reimer, P.J., et Reimer, R., 2000. CALIB radiocarbon calibration HTML version 5.0.2 and marine correction data base, <http://calib.qub.ac.uk/calib/>.
- Taylor, F.J.R. et Pollinger, U., 1987. Ecology of dinoflagellates. In: Taylor, F.J.R. (Eds.), *The biology of dinoflagellates*. Blackwell Scientific, Oxford, pp. 398-529.
- Telford, R.J., 2006. Limitations of dinoflagellate cyst transfer functions, *Quaternary Science Reviews* 25, 1375-1382.
- Versteegh, G.J.M., et Blokker, P., 2004. Resistant macromolecules of extant and fossil microalgae. *Phycological Research*, 52, 325-339.
- Walczowski, W., Piechura, J., Osinski, R. et Wieczorek, P., 2005. The West Spitsbergen Current volume and heat transport from synoptic observations in summer. *Deep-Sea Research Part I* 52(8), 1374-1391.